Implementation of a Droop Based Voltage Controller through an EV Charging Station in an Islanded Microgrid

A dissertation submitted in fulfillment of the requirements for the Degree

of

MASTER OF ENGINEERING

in

Power Systems

Submitted By

Shubhangi Jagota

Regd. No. : 801441028

Under the Guidance of

Mr. Shakti Singh

Assistant Professor, EIED

2016

Electrical and Instrumentation Engineering Department

Thapar University, Patiala

(Declared as Deemed-to-be-University u/s 3 of the UGC Act., 1956)

Post Bag No. 32, Patiala 147004

Punjab (India)

DECLARATION

I hereby certify that the work which is presented in dissertation entitled, "***Implementation of a Droop Based Voltage Controller through an EV Charging Station in an Islanded Microgrid***", in fulfillment of the requirements for the award of the degree of **Master of Engineering** in **Power Systems**, submitted to Electrical & Instrumentation Engineering Department of Thapar University, Patiala is as authentic record of my own work carried under the supervision of **Mr. Shakti Singh**. It refers others researchers work which are duly listed in the reference section. The matter contained in this dissertation has not been submitted, neither in part nor in full to any other degree to any other university or institute except as reported in text and references.

Place: Patiala
Date: 13-7-2016

Shubhangi

(Shubhangi Jagota)
Roll No.: 801441028

It is certified that the above statement made by the student is correct to the best of my knowledge and belief.

Shakti Singh

(Mr. Shakti Singh)
Assistant Professor
Electrical & Instrumentation Engineering Department
Thapar University, Patiala

Date: 13-7-2016

Countersigned by:

Agarwal

(Dr. Ravinder Agarwal)
Head
Electrical & Instrumentation Engineering Department
Thapar University, Patiala

SSBhatia

(Dr. S.S. Bhatia)
Dean (Academic Affairs)
Thapar University,
Patiala

CERTIFICATE

Certified that the dissertation entitled, "***Implementation of a Droop Based Voltage Controller through an EV Charging Station in an Islanded Microgrid***", which is being submitted by Shubhangi Jagota in fulfillment of the requirements for the award of the **Master of Engineering** in **Power Systems**, to Thapar University, Patiala, is a bona-fide record of the candidates own work carried out by her under my supervision and guidance. The matter contained in this dissertation has not been submitted, neither in part nor in full to any other university or institute for award of any degree.

Place: Patiala
Date: 13-7-2016

Shakti Singh

Mr. Shakti Singh

ABSTRACT

The rapidly depleting fossil fuels and growing needs for better efficiency and reliability of power supply in the present electrical network makes the concept of microgrids vitally important. Channelizing the elevation in the field of renewable energy sources (RESs) for the reformation of the existing power grids explain the essence of a microgrid. However, the variable nature of the renewable power produced is one of the prominent factors affecting the stability of the islanded microgrids. High incursions of RESs in islanded microgrids have raised many voltage issues in power systems. The voltage fluctuations owing to integration of RESs is a well identified phenomenon in microgrids. These fluctuations can be controlled through power electronics (PE) interfaces with energy storage systems (ESSs). However, installation of conventional ESS in microgrids is a costly affair. With recent developments in electric vehicles' (EVs') market and economic incentives provided by government, EVs have gained the potential to replace the traditional storage devices. This work proposes a microgrid, consisting of EVs to facilitate energy storage, as well as to provide voltage regulation support. A voltage controller based on active power/voltage, i.e., P/V droop characteristic has been modeled which regulate the voltage by injecting or drawing active power from the EVs charging station (CS). The desired active power regulation is achieved by controlling charging and discharging rates of EVs. Further, a control algorithm has been developed for optimal distribution of power among each EV, considering their individual charging/discharging requests. The suggested control scheme has been simulated and verified on a microgrid test system.

Keywords: *Active power, charging station, droop control, electric vehicles, energy storage systems, microgrid, renewable energy sources, voltage control.*

ACKNOWLEDGEMENT

I take the privilege to offer my deepest sense of gratitude to my supervisor **Mr. Shakti Singh**, for his understanding, encouragement and personal attention which have provided good and smooth basis for my dissertation tenure. I would also take this opportunity to thank **Dr. Mukesh Singh**. This work would not have been possible without his guidance, support and encouragement. Under his guidance I successfully overcame many difficulties and learned a lot.

I am also thankful to **Dr. Prakash Gopalan**, Director of Thapar University, Patiala for providing the facilities for the completion of M.E. I express my deep sense of gratitude towards **Dr. Ravinder Agarwal**, Head of the Department of Electrical & Instrumentation Engineering, Thapar University, Patiala for constantly encouraging each student to put their best foot forward in whatever field of work they take up, and **Ms. Manbir Kaur**, Associate Professor & PG Coordinator for her motivational approach.

I extend my gratitude to the researchers and scholars whose hours of toil have produced the papers that I have used in the dissertation. I further express my indebtedness to my parents who have constantly helped me keep my morale high all through the work.

Shubhangi

Shubhangi Jagota
801441028

TABLE OF CONTENTS

LIST OF FIGURES

LIST OF TABLES

LIST OF SYMBOLS

α	Phase angle of inverter output impedance.
a	Constant for quantity of load for active power.
$C_{rate_{ijk}}$	Charging/Discharging rate of i^{th} EV of j^{th} type and k^{th} category.
$C_{rate_{ij}}^{max}$	Maximum allowable charging/discharging rate of i^{th} EV of j^{th} type.
δ	Power angle.
δP	Power difference between generation and demand in microgrid.
Δt	Time interval at which proposed controller operates.
ΔP	Power injected into or drawn from microgrid.
ΔV	Voltage deviations at microgrid bus.
dP	Actual power distributed among EVs.
η_{ij}	Battery efficiency of i^{th} EV of j^{th} type.
E_{ijk}	Energy stored into or discharged from i^{th} EV of j^{th} type and k^{th} category.
E_{ijk}^{st}	Energy stored in i^{th} EV of j^{th} type and k^{th} category.
$E_{max_{ij}}$	kWh capacity of i^{th} EV of j^{th} type.
I_0	Inverter output current.
k	Represent category of EVs.
l	Determine behavior of load for active power.
n	Total number of EVs at CS.
n_A	Number of category A vehicles at CS.
n_B	Number of category B or dual mode EVs at CS.
n_C	Number of category C vehicles at CS.
P_0	Active power output of VSI.
P_{DG}	Power supplied by DG unit.
P_{DG_e}	Power supplied by DG unit to EVs.
P_{DG_m}	Power supplied by DG unit to microgrid.
$P_{DG_{rtd}}$	Power rating of DG unit.
P_i	Instantaneous PV power.
P_i^{EV}	Sum of power distributed among EVs.
P_{ijk}	Power injected or drawn from i^{th} EV of j^{th} type and k^{th} category.
$P_{ijk}^{in/dr}$	Power that can be injected or drawn from i^{th} EV of j^{th} type and k^{th} category.
$P_{ijk_{total}}^{in/dr}$	Total power that can be injected or drawn from EVs at CS.

P_l	Power requirement of load in microgrid.
P_{max}	Maximum power that can be injected into microgrid.
P_{min}	Maximum power that can be drawn from microgrid.
P_r	Rated PV power.
P_{ref}	Active power reference for microgrid.
P_{rtd}	Rated wind turbine power.
P_s	Power supplied to load by microgrid.
P_w	Instantaneous wind turbine power.
Q_0	Reactive power output of VSI.
R_0	Line and inverter output resistance.
R_i	Instantaneous solar radiations.
R_r	Rated solar radiations.
s	Wind speed.
s_{cin}	Cut-in wind speed.
s_{cout}	Cut-out wind speed.
s_{rtd}	Rated wind speed.
SOC_{ijk}	Initial SOC of i^{th} EV of j^{th} type and k^{th} category.
SOC^d_{ijk}	Desired SOC by i^{th} EV of j^{th} type and k^{th} category.
$SOC_{max_{ij}}$	Maximum allowable SOC for i^{th} EV of j^{th} type.
$SOC_{min_{ij}}$	Minimum allowable SOC for i^{th} EV of j^{th} type.
$t_{e_{ijk}}$	Departure time of i^{th} EV of j^{th} type and k^{th} category.
$t_{s_{ijk}}$	Arrival time of i^{th} EV of j^{th} type and k^{th} category.
V_{max}	Maximum voltage at microgrid bus.
V_{min}	Minimum voltage at microgrid bus.
V_r	Magnitude of fundamental frequency component of VSI output voltage.
V_{ref}	Voltage reference for microgrid bus.
V_s	Real time voltage at microgrid bus.
x	Enhanced voltage at microgrid bus.
X_0	Line and inverter output inductance.
Z_0	Line and inverter output impedance.

LIST OF ABBREVIATIONS

BESS	Battery Energy Storage Systems
BEV	Battery Electric Vehicle
CHP	Combined Heat and Power
CS	Charging Station
DG	Diesel Generator
D-STATCOM	Distribution Static Compensator
ESS	Energy Storage Systems
EV	Electric Vehicle
FACTS	Flexible ac Transmission Systems
HEV	Hybrid Electric Vehicle
LV	Low Voltage
MV	Medium Voltage
PCC	Point of Common Coupling
PCS	Power Control Switch
PDCU	Power Distribution Control Unit
PE	Power Electronics
PHEV	Plug-in Hybrid Electric Vehicle
PV	Photovoltaic
P/V	Active power/Voltage
PWM	Pulse Width Modulation
RES	Renewable Energy Sources
SOC	State of Charge
STATCOM	Synchronous Compensator
UPQC	Unified Power Quality Conditioner
VSC	Voltage Source Converter
VSI	Voltage Source Inverter

Chapter 1

INTRODUCTION

1.1 Microgrid

Microgrids are emerging as a boon in incorporating the idea of smart grid in the present power system. It can be viewed as a solution to various challenges for both consumers and conventional grids in terms of stability, reliability, flexibility and environment issues [1]. Basically, a microgrid is a group of loads being fed by a low voltage (LV) distribution network, which functions as a single controlled system. A typical layout of an ac microgrid is shown in Fig. 1.1. It primarily consists of distributed microsources, energy storage systems (ESS) and power electronics (PE) interfaces [2]. A microgrid may be categorized as AC microgrid and DC microgrid based on the nature of the power being fed to the load. In AC microgrids, alternating nature of power is fed to the load, while DC power is supplied to the load in a DC microgrid. DC microgrids have many advantages as there is no need of synchronization, frequency and reactive power regulations. However, AC microgrids are preferred as most of the load is AC in nature. The main remunerative aspects of microgrids are listed as follows [3].:

- Reduced load on the grid.
- Reduced transmission and distribution losses.
- High efficiencies.
- Low emission microsources.

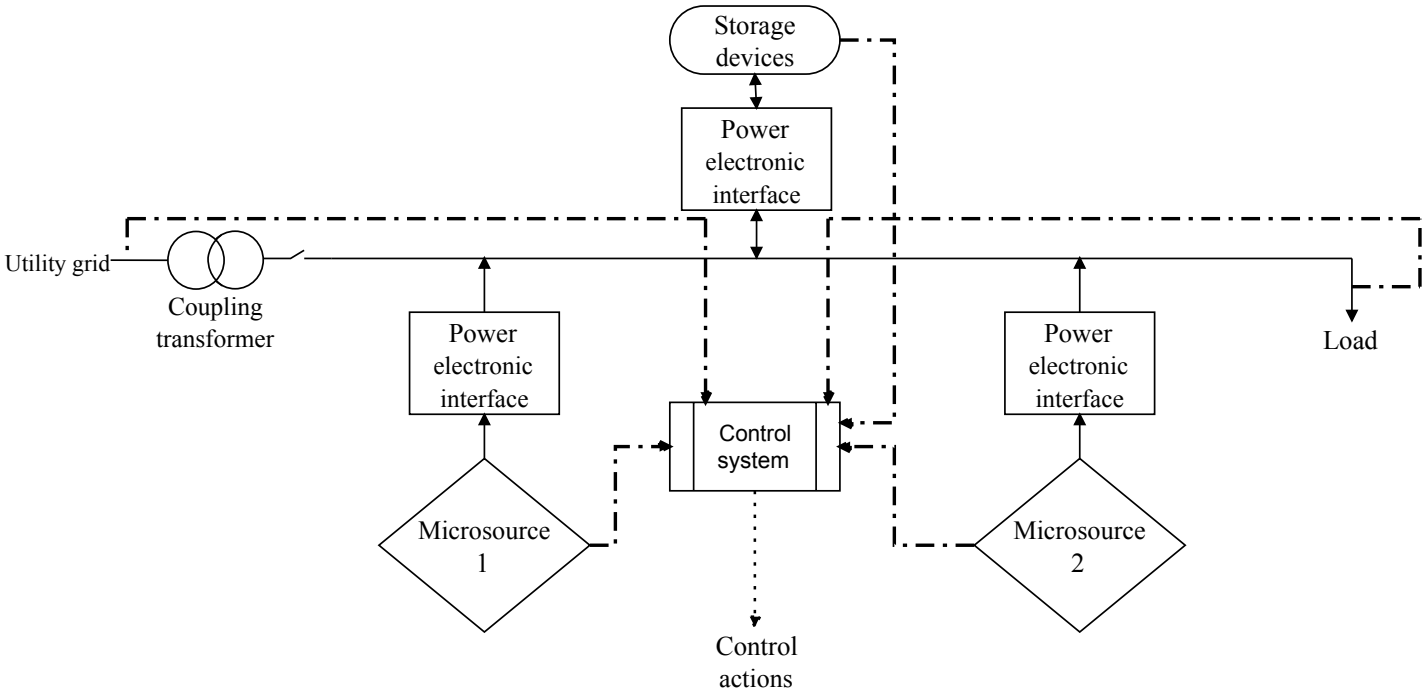

Figure 1.1: Layout of a typical AC microgrid

- Enhanced reliability of power during blackouts.
- Provision of combined heat and power (CHP) operations.

Microsources mainly consist of renewable energy sources (RESs) with low output power, low voltage (less than 480V at load side feeder) and negligible CO_2 emissions [4]. Renewable energy can be harnessed from natural sources such as sun, wind turbines, biomass, geothermal energy, hydrogen and fuel cells, etc. Amidst all of above mentioned sources of energy, sun, wind and fuel cells are mostly used in microgrids. Solar energy can be harnessed through photovoltaic panels, solar heaters, solar thermal power plants. However, photovoltaic (PV) panels and wind turbines are used at large scale to harvest the solar and wind energy respectively. These microsources are preferred due to their abundant quantity, and low pollution nature. Besides being clean, their integration is appreciated as they have scope of generation where conventional generation is not accessible. Thus, integration of RESs in microgrids provide a solution for reliable electricity in remote and off-grid areas [5].

Although there are various advantages of RESs, there are also few challenges in their integration in microgrids. The unpredictable and irregular nature of these sources raises major issues

effecting the efficiency, security and stability of the microgrid systems. As there is a wide scope for RESs in present power system, the intermittency associated with them needs to be addressed. To cope up with variable nature of RESs, storage devices like battery energy storage systems (BESS), supercapacitors, flywheels, electric vehicles (EVs) has been a prime topic of research among researchers [6]. With support of the government worldwide and advancements in the field of battery technology, EVs have secured a remarkable growth in upcoming years. High fuel efficiencies, incentives provided by government and environment friendly nature are the prime reasons why EVs will completely replace other storage devices in the coming time. EVs can be broadly classified as Plug-in Hybrid EVs (PHEVs), Hybrid EVs (HEVs) and Battery EVs (BEVs). Among all, PHEVs and BEVs are studied by researchers mostly as they can be integrated into grids [7]. Apart from microsources and storage systems, controllers are also needed to be incorporated in microgrid. The controller regulates the operation of power electronics interfaces in the microgrid for maximizing its efficiency and maintaining the security of supply [8].

Microgrids have the following two modes of operations:

- Grid connected mode
- Islanded mode

In grid connected mode of operation, a microgrid is connected to the utility grid through a point of common coupling (PCC) through an isolating switch as shown in Fig. 1.1. During this mode, the power is exchanged between both the microgrid and utility grid. The islanded mode of operation may be intentional or non-intentional. An islanded microgrid functions independent from utility grid and no power is exchanged between the two. During grid connected mode, any power deficit event in the microgrid can be avoided by importing power from the host grid. On the contrary there is no external source of power in a stand-alone microgrid and the power balance has to be maintained by the microgrid itself [3].

1.2 Voltage issues in islanded microgrids

Unlike grid connected microgrids, there is no external source of power in an isolated microgrid and the power balance has to be maintained by the microgrid itself. As microgrid functions

independent from the utility grid during islanded mode, no external power source is present. Thus, maintaining regularity of power supply at consumer's end is a challenging work in isolated microgrids. A failure in balancing the demand and supply at any instant can result in frequency and voltage deviations in the microgrid [9]. The effects of voltage deviation are more profound as it may cause serious disturbances and power outages in low voltage networks [10]. Lack of voltage control in microgrids may result in high circulating currents and supply of low quality power to the consumers [11], [12].

Fluctuating nature of load and power generation are the main causes behind voltage variations in an islanded microgrid integrated with RESs. As RESs depend upon nature for their operation, power generated through them is unpredictable in nature. This may lead to instances of generation demand mismatch causing serious voltage problems in microgrid. Any increase in demand supply gap directly effects the voltage of the network. While an increase in load beyond generation decreases the voltage below the nominal voltage, decrease in load results in an increase in voltage. This increase or decrease in microgrid's voltage further effects stability of the system and power supply to the load. To ensure an efficient operation of an islanded microgrid with respect to voltage control, the operation of PE interfaces is regulated. The power electronics devices integrated in microgrids are often controlled to ensure a reliable operation during islanded mode.

1.3 Literature Survey

The alleviation of voltage variations in microgrid has been a prime topic of discussion among various researchers. Different techniques have been proposed for voltage control in microgrids to stabilize their operation. Flexible alternating current transmission system (FACTS) devices have been investigated for mitigating voltage deviations through reactive power support. A voltage imbalance control in a microgrid through regulating reactive power have been discussed by Majumder [13]. The author suggested a distribution static compensator (D-STATCOM) based control strategy, for a microgrid with high penetration of distributed generators. The basic idea was to control both distributed generators and D-STATCOM in order to prevent voltage sags in the microgrid. The author proposed a communication loop based control strategy to achieve voltage regulations. Although, the suggested technique mitigated voltage sags in the system to an appreciable limit,

the effect of RESs integration on microgrid voltage was not considered. In a similar work, a D-STATCOM based model have been discussed by an author for voltage control in a microgrid [14]. The authors employed the control scheme to vary the positive and negative sequence voltage of the microgrid . The authors suggested the control scheme to achieve the positive sequence voltage equal to the rated value. Further, the suggested scheme also took care of the negative sequence voltage by decreasing it to a tolerable value. The control scheme utilized reactive power support for voltage regulations. In a similar approach, application of unified power quality conditioner (UPQC) was discussed for voltage compensation in microgrids [15]. The suggested scheme provided reactive power compensation for the purpose of voltage control. The authors considered the operation of the microgrid in grid-connected mode as the microgrid functioned connected to the utility grid. The suggested control scheme was designed to compensate both microgrid and grid side bus voltages. The authors suggested the application of the control structure to mitigate both increase and decrease in voltage of the system. The authors described the dual function of UPQC as STATCOM and typical UPQC for compensating voltage variations at grid side and microgrid side respectively. However, the authors did not discourse its applicability in an isolated microgrid system. Also, application of FACTS devices needs a complex control structure for their operation. In contrast to this, droop control is relatively a less complex technique as it does not involve complex communication networks [16]. Many researchers have suggested the employment of droop control for keeping the voltage fluctuations within required limits. Lopes *et al.* [17] investigated control schemes for reliable operation in standalone microgrids. The authors proposed a control scheme employing droop control in an isolated microgrid to compensate voltage variations. The control was employed through voltage source inverter (VSI) incorporated in the microgrid. Active power/frequency, i.e., P/f and reactive power/voltage, i.e., Q/V droop control were suggested for limiting frequency and voltage deviations respectively. The authors suggested to vary frequency and voltage of system by varying active power and reactive power respectively. However, due to high resistance to inductance ratio at low or medium voltage distribution networks, active power regulations are preferred for limiting voltage variations. Thus, the suggested control scheme is not relevant in an LV microgrid network. In another work, Sao *et al.* [18] proposed a droop based control for a microgrid integrated with converters. The authors suggested utilization of multiple voltage source converters (VSCs) operating parallely in a microgrid. Voltage - power droop/frequency

- reactive power boost, i.e., VPD/FQB control strategies were discussed. The authors suggested employment of individual droop control for each VSC to provide voltage and frequency regulation. Reactive power compensation was utilized by the authors for controlling frequency of the microgrid. The authors suggested the application of control scheme for both islanded and grid connected mode. However, the authors have not accounted the power management aspect in this work. In addition to it, the modeling of VSC interfaces in power sources and ESS was not distinguished while designing the control scheme.

Many of the existing proposals have overlooked PE interfaces in ESS for voltage control in microgrids. Nonetheless, storage systems can efficiently regulate the voltage by supporting a microgrid during peak demands and events of low power generation [19]. In view of this, a voltage control technique based on optimal reference schedule for a smart grid has been suggested by Ziadi *et al.* [20]. The smart grid was considered to be having high integrations of PV generation. The authors discussed the control scheme for BESS, loads and distributed generators. The control scheme was designed to maintain the microgrid voltage within limits. Moreover, the authors also suggested the incorporation of controlled loads in a distribution network in order to achieve better efficiency. The effect of large penetrations of RES on the voltage of microgrid are considered while designing the control structure. However, the control strategy developed has considered only a single PV source, therefore its feasibility in a multi-source microgrid cannot be evaluated. In [21] stability of a microgrid was investigated with respect to voltage and frequency. The authors suggested a control scheme for ESS in order to control voltage and frequency variations in the system. The voltage and frequency of the microgrid have been suggested to vary through a droop controlled ESS. Both the voltage and frequency are regulated through droop coefficients. The authors have considered islanded operation of the microgrid while designing the control structure. Moreover, the authors have also considered the essence of demand-supply balance in an islanded microgrid. However main focus of the author was on frequency regulation rather than voltage control. In a different context, a cooperative control scheme for ESS to regulate voltage and frequency of a microgrid was presented in [22]. The control scheme employs primary and secondary control system to achieve a stable operation during islanded mode of operation. Most of the existing microgrid structures considered by different authors employ BESS for energy storage. As EVs provide better performance than BESS with respect to economy and maintenance, control aspects for voltage

through EVs needs to be studied. Working in this direction, Falahi *et al.* [23] have presented a control scheme employing voltage drop compensation in a distribution grid, through reactive power injection by EV chargers. Although, the suggested scheme was effective in controlling voltage drops, it did not account for charging/discharging requests by EVs' users. In another work, reactive power and voltage support potential of EVs parked at a charging station (CS) was compared to a STATCOM [24]. The authors employ reactive power compensations in order to limit the voltage of the system within limits. However, voltage variations by regulating active power injections through CS were not accounted.

1.4 Research Gap

It can be inferred from the literature survey that voltage control in islanded microgrids integrated with RESs needs to be investigated. In reference [13], [14] and [15], D-STATCOM and UPQC were investigated by authors, in order to control voltage in microgrids. However, droop control is a more simpler technique for achieving efficient voltage regulations through PE interfaces incorporated in microgrids. In [18], the authors suggested voltage control in microgrids through droop controlled VSCs. However, PE interfaces in power sources were not differentiated from PE interfaces in energy storage. ESS can be utilized for regulating power by optimal management of energy in a microgrid. Thus, voltage regulating potential of ESS needs to be investigated. Voltage control though BESS in a microgrid with large integration of PV power was discussed in [20]. Similarly, a frequency and voltage regulation scheme through BESS was investigated for an islanded microgrid in [21]. However, as EVs are better than BESS with respect to performance, there is a need to investigate application of EVs for voltage control in microgrids. In view of this, voltage compensation potential of EV chargers was discussed in [23]. In a similar work, the operation of EVs at a park was compared to STATCOM for providing voltage support through reactive power compensation [24]. However, due to high R/X ratio in an LV network, voltage of the system varies with active power. Thus, there arises a need to design a voltage controller employing active power/voltage, i.e., P/V droop control characteristics.

1.5 Motivation and Objectives

It can be concluded from the literature survey that most of voltage compensation techniques for microgrids involve complex control schemes. A very less work done employing droop characteristics utilizes inverter interfaces in power sources only. A very limited work is found in literature, with respect to voltage regulations through ESS. A few control schemes considering ESS have concentrated on static battery units. In addition to it, majority of the approaches employing EVs still emphasized on voltage control by considering the effect of reactive power. However, in an LV microgrid network, active power compensation has significant role in effecting voltage of the system. Thus, there is a need to incorporate a controller that regulates the voltage of the microgrid through regulating active power. A P/V droop voltage controller is proposed in this work for providing voltage support to the microgrid. Moreover, most of the existing works have neglected the inclusion of power management aspect while designing the voltage control schemes. To maintain the power balance, there should be an optimal charging schedule for distribution of power among individual EVs while taking care of their charging/discharging needs as well. Moreover, the voltage controller should involve the effects of various RESs, load and the dynamics of EVs.

1.5.1 Objectives

In view of the aforementioned discussion, the major objectives of this work have been listed below:

- Development of a reliable voltage control scheme for an islanded microgrid integrated with RESs, which employs active power/voltage i.e., P/V droop characteristics to inject or draw active power from a CS.
- Employment of P/V droop characteristics for optimal power distribution among each EV available at CS, to maintain a constant nominal voltage, as well as fulfill the charging/discharging needs of the EVs.
- Efficient utilization of EVs such that they serve as either distributed energy source or load, to provide peak shaving or valley filling respectively, thus minimizing demand-supply gap simultaneously.

Chapter 2

SYSTEM DESCRPITION

An ac microgrid feeding a cluster of loads, able to operate in both grid connected and islanded mode is considered. However, the main focus of the proposed work is on voltage control during isolated operation. The microgrid consists a PV unit and a wind generation unit for the purpose of of power generation. To deal with the intermittent nature of generation units, EVs are integrated in the microgrid as ESS which gets charged and discharged through a CS. A diesel generator (DG) unit is also installed as a backup power source for enhancing reliability of the microgrid. In addition to this, a control system is also integrated in the microgrid to regulate the charging/discharging actions of the EVs to maintain the desired voltage at the bus.

2.1 Microgrid architecture

Fig. 2.1 shows schematic diagram of an AC microgrid feeding a load with fluctuating demand profile. The microgrid is assumed to be an LV distribution network, thus possessing resistive nature. It is connected to the utility grid at point of common coupling (PCC) through an 11kV/400V step down transformer. The microgrid can operate in either grid connected or islanded mode of operation. However, this paper investigates isolated operation of microgrid to realize the application of proposed system in off grid locations. The islanded mode of microgrid is observed by opening the isolating switch, as shown in the figure. A PV and a wind generation unit act as a primary source of power generation. As solar and wind power is unpredictable in nature, a 50 kW DG unit is installed as backup power source for supporting the microgrid during emergencies, such as

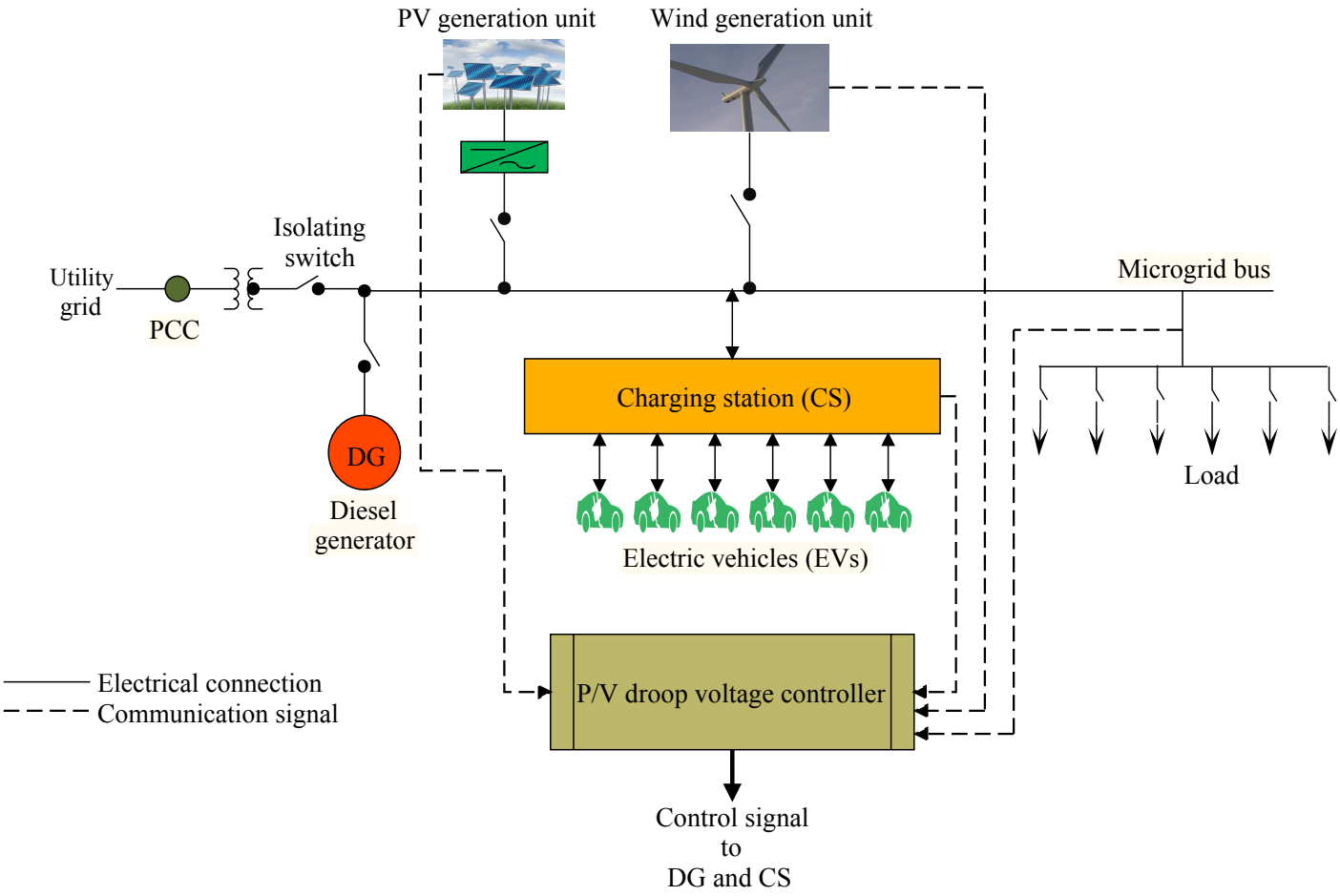

Figure 2.1: Schematic diagram of proposed microgrid

breakdown of both primary power generating sources. Apart from it, EVs are integrated as ESS which gets charged and discharged through a CS at the microgrid. The CS has the capacity to accommodate 30 EVs at any given time. All the above mentioned installations including generation units, power electronics devices, and CS are connected through a common AC bus. To limit any voltage fluctuations at the bus, a P/V droop voltage controller is incorporated which regulates active power between EVs and microgrid. The CS plays a vital role in regulating microgrid's voltage and is described as follows.

2.2 Charging Station (CS)

Fig. 2.2 depicts the block diagram of EV charging station installed in the proposed microgrid. It consists of a DC/DC converter for each EV, DC/AC inverter and charging bays. To facilitate power

flow between EVs and microgrid, pulse width modulation (PWM) based voltage source inverter (VSI) is installed at CS. Fig. 2.3 shows an equivalent circuit of VSI connected at the microgrid bus. As shown in figure, I_0 is the inverter output current and $Z_0\angle\alpha$ represents magnitude and phase angle of both line and inverter output impedance. As the proposed microgrid is assumed to be an LV distribution network, impedance Z_0 will be resistive due to high R_0/X_0 ratio. Accordingly, active and reactive power through VSI can be determined as follows.

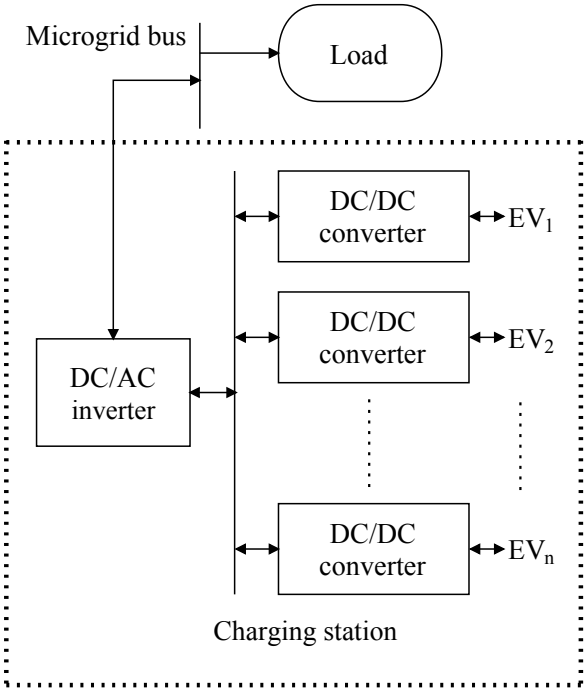

Figure 2.2: Block diagram of charging station.

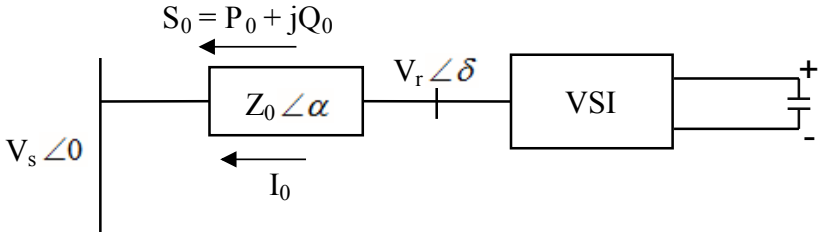

Figure 2.3: Equivalent circuit of a VSI connected at microgrid bus [25].

$$P_0 \equiv \frac{V_s(V_r - V_s)}{R_0} \tag{2.1}$$

$$Q_0 \equiv \frac{-V_s V_r \delta}{R_0} \tag{2.2}$$

In above equations, P_0 and Q_0 denotes the active and reactive power through VSI. V_s is the voltage magnitude of the microgrid bus, V_r is the magnitude of the fundamental frequency component of the VSI output voltage, and R_0 is line and output resistance of the VSI. δ is the power angle and assumed to be negligibly small. It can be inferred from Eq. (2.1) and Eq. (2.2) that the active power can be varied with voltage difference $(V_r - V_s)$ and remains constant with change in δ [26]. Consequently, by varying active power flow between EVs and microgrid through VSI, efficient voltage regulations can be achieved at the microgrid bus.

2.3 Electric Vehicles (EVs)

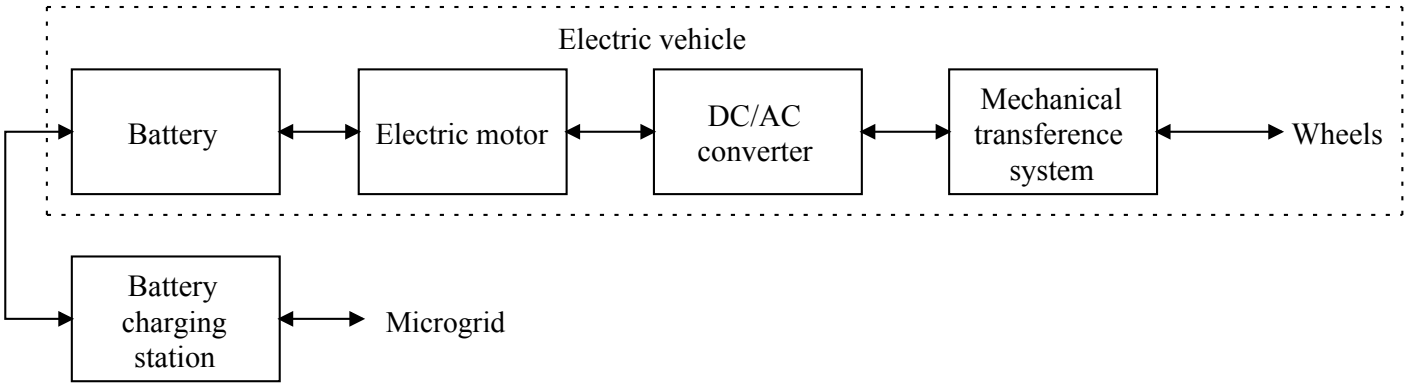

Figure 2.4: Diagrammatic representation of EV system [27]

Electric vehicles, as the name suggests are powered through battery operated electric motors. Fig 2.4 shows a diagrammatic representation of a typical EV system [27]. The main components include a battery pack, electric motor, a dc/ac converter and mechanical transference system to transmit the mechanical power to the wheels. The batteries are charged through charging cables at charging stations and the electric power is acquired through the power grids [28]. With extensive promotions received by EVs throughout world, their market is bound to deploy in the coming future. EVs have an edge over conventional vehicles, as they brings down the CO_2 emissions. The environmental benefits of EVs will be increasing with time as and when the penetration of cleaner RES in the power sector increases. Moreover, they can be utilized as distributed ESS, thus playing a significant role in maintaining the stability of a microgrid. EVs can enhance the performance of a microgrid by providing ancillary services like voltage and frequency regulation, peak shaving,

and valley filling. Therefore, EVs are ideal to be integrated as ESS in a stand-alone microgrid.

Keeping the above aspects in view, the proposed microgrid is equipped with EVs to provide voltage regulation as well as energy storage facility. For any i^{th} EV present at the CS at time instant t, energy $E_i^{st}(t)$ stored in its battery can be given by following equation.

$$E_i^{st}(t) = \frac{E_{max_i}}{100} SOC_i(t) \tag{2.3}$$

where, E_{max_i} kWh capacity of i^{th} EV and $SOC_i(t)$ refers to the state of charge (SOC) of the corresponding EV's battery. Further, the charging and discharging mechanism of EVs is subjected to the following constraints:

$$SOC_{min_i} \leq SOC_i(t) \leq SOC_{max_i} \tag{2.4}$$

$$C_{rate_i}(t) \leq C_{rate_i}^{max} \tag{2.5}$$

where, $C_{rate_i}(t)$ denotes charging/discharging rate of the i^{th} EV at time t. SOC_{min_i} and SOC_{max_i} refers to minimum and maximum allowable SOC limits respectively. The SOC limits and $C_{rate_i}^{max}$ are user specified and should not be violated while charging/discharging of EVs. Further, EVs arriving at the CS are divided into three types, as represented in Table 2.1.

Table 2.1: Types of EVs' batteries and their specification

Type	E_{max} (kWh)	SOC_{min} (%)	η	C_{rate}^{max}
Type I	4	20	0.95	3
Type II	6	25	0.9	3.5
Type III	8	30	0.85	4

Chapter 3

METHODOLOGY ADOPTED

The proposed microgrid consists of a PV and a wind generation unit for generating electrical power. These microsources depend upon environmental factors for their operation, which results in intermittent nature of output power. The power generated by PV panels is greatly dependent on the solar radiations, and is determined as follows [29].

$$\frac{P_i}{P_r} = \frac{R_i}{R_r} \tag{3.1}$$

where, P_i is power generated corresponding to solar radiations R_i and P_r refers to the rated power of the array at rated solar radiations R_r. Due to uncertain solar radiations, PV power possesses variable nature. This results in voltage variations at the bus to which the PV panels are connected. It is evident from Fig. 3.1 that the voltage deviations increase with the increased penetration of PV power in a LV or medium voltage (MV) distribution system. In a similar manner, wind power is a function of wind speed which can be illustrated as follows [30].

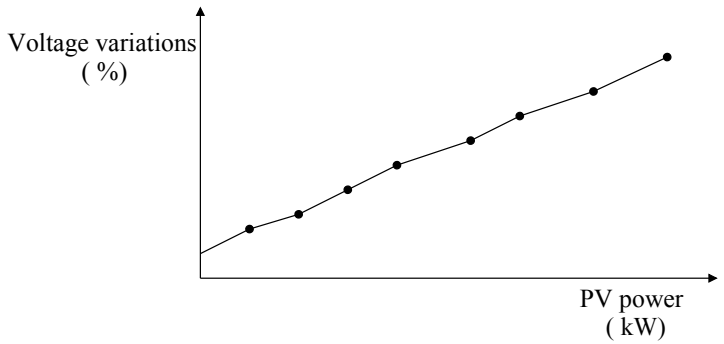

Figure 3.1: Voltage variations due to increasing PV power in a LV distribution system [31].

$$P_w = \begin{cases} 0 & 0 \leq s < s_{cin} \\ P_{rtd}[A' + B's + C's^2] & s_{cin} \leq s < s_{rtd} \\ P_{rtd} & s_{rtd} \leq s \leq s_{cout} \\ 0 & s > s_{cout} \end{cases} \tag{3.2}$$

where, P_w is the wind power corresponding to wind speed s. Here, A', B' and C' are constants, and demonstrated in [29]. s_{cin} and s_{cout} are the cut-in and cut-out wind speeds respectively, while s_{rtd} is rated wind speed at which rated power P_{rtd} is delivered. Fig. 3.2 shows the output power generated through a wind power generating station as a function of wind speed.

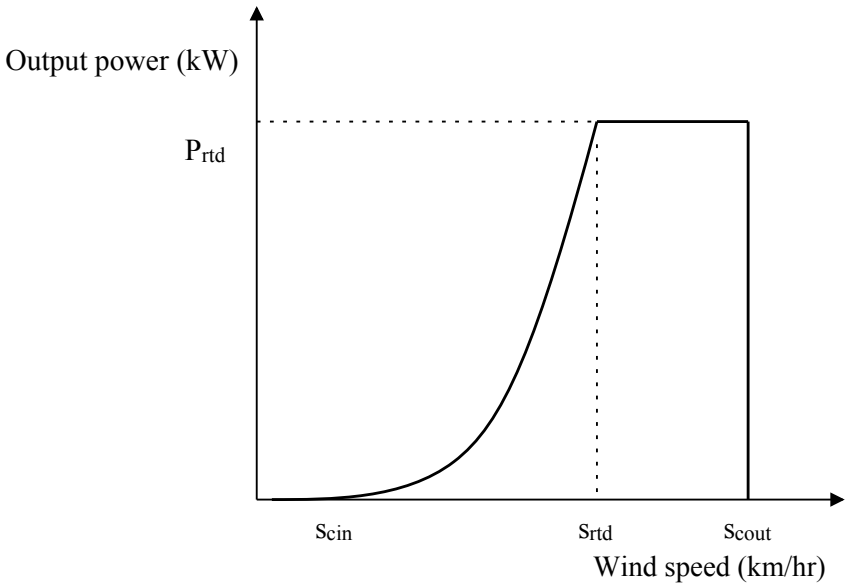

Figure 3.2: Wind power generation vs wind speed [32].

Besides generation, load characteristics are also an important aspect for reliable operation in an isolated microgrid. It is important to maintain the balance between demand and supply in a distribution network for stability of the system. The inability to maintain this balance leads to voltage variations in the microgrid causing instability [33]. A basic P-V curve is shown in Fig. 3.3 depicting the relation between the magnitude of the load bus voltage and the active power supplied to the load. The point O is generally referred as a nose point or a critical point. An operation beyond the nose point results in voltage instability or collapse [34]. The variation of load power

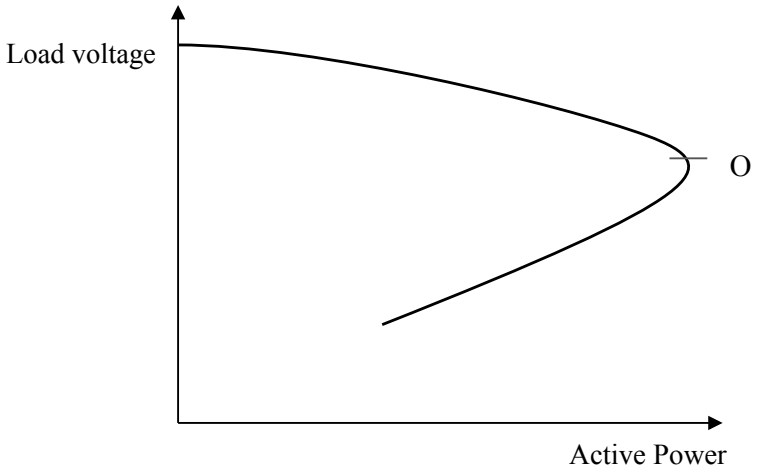

Figure 3.3: Basic load P-V curve [35]

with voltage can be summarized by considering static load model given as

$$\frac{P}{P_{rt}} = a\left(\frac{V}{V_{rt}}\right)^{l} \tag{3.3}$$

where, P_{rt} and V_{rt} are the rated active power and voltage, a determines the given load's quantity and l represents the behavior of load for active power [36]. The equation shows that the load voltage is directly effected by any change in the active power supplied to it.

If P_s and P_l are the power supplied to a load in a microgrid and the power requirement of the load respectively, then the polarity of δP will decide any increase or decrease in the voltage at load bus. Here δP is the difference between P_s and P_l which can be represented as

$$\delta P = P_s - P_l \tag{3.4}$$

If the polarity of δP is positive then the load voltage will increase from the nominal value while a negative δP represents decrease in the load voltage.

3.1 P/V droop voltage controller

In order to accomplish an efficient control of inverters interfaced with ESS in microgrid, droop control is the most appropriate technique. This technique is derived from the primary frequency regulation criteria employed for generators in power system. It does not require complex com-

munication network which makes the control more flexible and reliable. The control is designed according to parameters acquired at terminals of the inverters [16]. In accordance with droop control characteristics, this work proposes a voltage control technique by regulation of active power through VSI. The block diagram of the control scheme for the proposed P/V droop voltage controller is represented in Fig. 3.4. The developed scheme employs two control units, explained as follows.

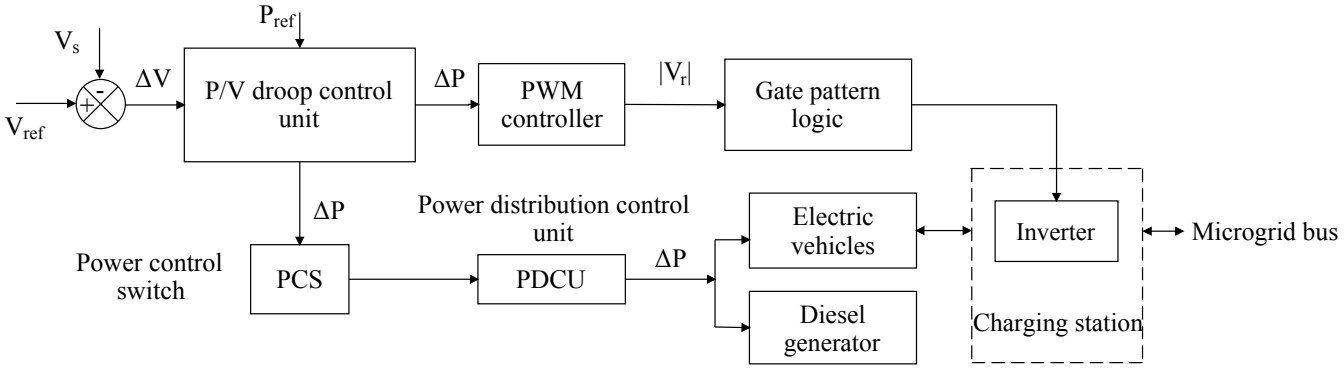

Figure 3.4: Proposed control scheme for VSI and EVs at CS.

3.1.1 P/V Droop Control Unit

This control unit employs classic P/V droop characteristics as shown in Fig. 3.5. The real time voltage V_s at the microgrid bus is compared with the reference voltage V_{ref}. The difference ΔV is fed to the P/V droop control unit, along with the set power reference P_{ref}. Further, the working of the P/V droop control unit is explained through algorithm 1, demonstrated as follows.

Algorithm 1 Computation of ΔP employing P/V droop characteristics

Input: $\Delta V(t), V_{ref}, V_{max}, V_{min}, P_{ref}, P_{max}, P_{min}$
Output: Power ΔP to be injected into or drawn from the CS respectively.

1: Store $\Delta V(t), V_{ref}, V_{max}, V_{min}, P_{ref}, P_{max}, P_{min}$
2: **for** $(t = 1, t \leq 24, t++)$ **do**
3: **if** $(\Delta V(t) = 0)$ **then**
4: $\Delta P = 0$
5: PCS off
6: **else if** $(\Delta V(t) > 0)$ **then**

Compute $\Delta P_0 = P_{max} - P_{ref}$
Compute $\Delta P = \frac{\Delta P_0}{V_{ref} - V_{min}} \Delta V$
PCS on
else if $(\Delta V(t) < 0)$ **then**
Compute $\Delta P_0 = P_{ref} - P_{min}$
Compute $\Delta P = \frac{\Delta P_0}{V_{max} - V_{ref}} \Delta V$
PCS on
end if
end for

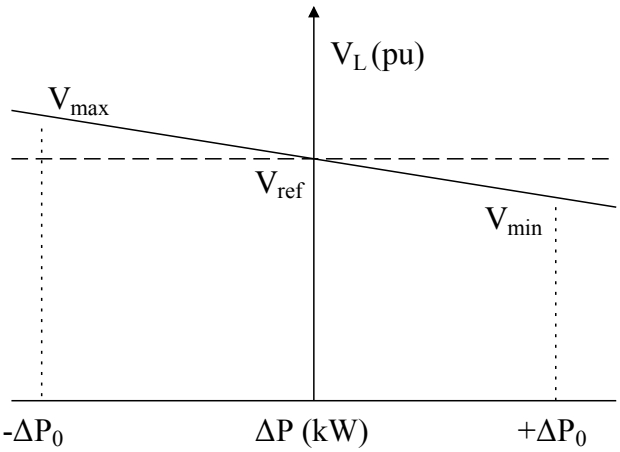

Figure 3.5: Classic model of P/V droop characteristics [25].

The suggested control algorithm provides power ΔP to be injected into or drawn from CS, respectively. The direction of ΔP is determined by polarity of ΔV resulting in three cases, described as follows.

- Case I ($\Delta V = 0$): In this case, the output of the controller ΔP is zero. Thus, no power is exchanged between microgrid and EVs. However, power control switch (PCS) shown in Fig. 3.4 is switched on, in order to facilitate power flow between EVs seeking charging and discharging, respectively.

- Case II ($\Delta V > 0$): During this case, V_s drops below the nominal voltage. Thus, the voltage difference $(V_{ref} - V_s)$ is positive. This results in positive ΔP, which indicates need to inject active power into the bus. Thus, PCS switches on and EVs inject required power into the microgrid.

- Case III ($\Delta V < 0$): This case includes an increase in V_s, which indicate the voltage difference

$(V_{ref} - V_s)$ to be negative. Thus, there arises a need to draw active power from the microgrid. This results in negative ΔP. Subsequently, PCS will be switched on leading to charging of EVs.

Further, output of the P/V droop control unit, ΔP is fed to the power distribution control unit (PDCU) through PCS, as shown in Fig. 3.4.

3.1.2 Power distribution control unit (PDCU)

A finite ΔP results in triggering PCS, which initializes PDCU to distribute ΔP among each EV and DG unit through a control algorithm. Here, all EVs are assumed to be having 100% SOC_{max}. For charging/discharging of i^{th} EV at instant t, the information with respect to $SOC_i(t)$, $C^{max}_{rate_i}$, t_{s_i}, t_{e_i}, and desired SOC i.e., $SOC^d_i(t)$ is provided by its respective owner. t_{s_i} and t_{e_i} are starting and ending time for charging/discharging of i^{th} EV respectively. For ease of power distribution, EVs present at CS are categorized based on their SOC. The EVs are categorized as category A, category B and category C having SOC (0 - 40)%, (40 - 70)%, and (70 - 100)%, respectively. Category B EVs are dual mode EVs which offers both charging and discharging of their batteries. During charging of EVs, it is assumed that at any instant t sufficient number of EVs are present at the CS to draw the required power from the microgrid, i.e.,

$$P^{in}_{ijk_{total}}(t) \geq \Delta P \qquad \forall k \in A, B \tag{3.5}$$

where, $P^{in}_{ijk_{total}}(t)$ is the maximum power which can be injected in EVs of category A and B available at the CS, and can be determined from following equation. Here, k represents the category of EVs.

$$P^{in/dr}_{ijk_{total}}(t) = \sum_{i=1,j=1}^{n(t),3} P^{in/dr}_{ijk}(t) \qquad \forall k \in A, B, C \tag{3.6}$$

$$P^{in/dr}_{ijk}(t) = \frac{E_{ijk}(t)}{t_{e_{ijk}} - t_{s_{ijk}}} \tag{3.7}$$

In Eq. (3.7), $P^{in/dr}_{ijk}(t)$ is total power that can be injected to/drawn from the i^{th} EV of j^{th} type at time t. $E_{ijk}(t)$ represents corresponding total energy that can be discharged or stored into respective

EV's battery, and is determined from following equation.

$$E_{ijk}(t) = \begin{cases} \frac{1}{\eta_{ij}} * E_{max_{ij}}[SOC^{d}_{ijk}(t) - SOC_{ijk}(t)] & charging \\ \eta_{ij} E_{max_{ij}}[SOC_{ijk}(t) - SOC^{d}_{ijk}] & discharging \end{cases} \tag{3.8}$$

Algorithm 2 Power distribution control

Input: Type, SOC_{ij} and user specified charging requests of EVs at CS of microgrid, ΔP.

Output: **Charging/Discharging schedule of EVs for 24 hours; Output power of DG unit across 24 hours.**

$\Delta t = 0.25$
for $(t = 0,\ t \leq 24,\ t + \Delta t)$ **do**
    Store charging/discharging requests by EV owners
    Register $n(t),\ SOC_{ij}(t),\ \Delta P(t)$
    Sort $n(t)$ in $n_A(t)$, $n_B(t)$, $n_C(t)$
    for (k = A,B,C) **do**
        Compute $P^{in/dr}_{ijk}(t),\ E_{ijk}(t),\ C_{rate_{ijk}}(t)$, using Eq. (3.7), Eq. (3.8), and Eq. (3.9) respectively.
        if $(C_{rate_{ijk}}(t) \geq C^{max}_{rate_j})$ **then**
            $C_{rate_{ijk}}(t) = C^{max}_{rate_j}$
            $P^{in/dr}_{ijk}(t) = C_{rate_{ijk}}(t) * E_{ijk}(t)$
        end if
    end for
    if $(\Delta P(t) > 0)$ **then**
        if $(P^{dr}_{ijC_{total}}(t) \leq \Delta P(t))$ **then**
            $P_{ijC}(t) = P^{dr}_{ijC}(t)$
            if $(P^{dr}_{ijB_{total}}(t) \leq \Delta P(t) - P^{dr}_{ijC_{total}}(t))$ **then**
                $P_{DG_m}(t) = \Delta P(t) - P^{dr}_{ijC_{total}}(t) - P^{dr}_{ijB_{total}}(t)$
                if $(P^{in}_{ijA_{total}}(t) \leq P_{DG_{rtd}} - P_{DG_m}(t))$ **then**
                    $P_{ijA}(t) = P^{in}_{ijA}(t)$
                    $P_{DG_e}(t) = P^{in}_{ijA_{total}}(t)$
                else
                    $P_{DG_e}(t) = P_{DG_{rtd}} - P_{DG_m}(t)$
                    $dP(t) = P_{DG_e}(t)$; Compute $P_{ijA}(t)$, using Eq.(3.10).
                end if
                $P_{mg}(t) = P_{DG_m}(t) + P^{dr}_{ijC_{total}}(t) + P^{dr}_{ijB_{total}}(t)$
                $P_{DG}(t) = P_{DG_m}(t) + P_{DG_e}(t)$
                $P_{ijB}(t) = P^{dr}_{ijB}(t)$
            else
                $P_{mg}(t) = \Delta P(t)$
                if $(P^{in}_{ijA_{total}}(t) \leq P^{dr}_{ijB_{total}}(t) - \Delta P(t) + P^{dr}_{ijC_{total}}(t))$ **then**
                    $P_{ijA}(t) = P^{in}_{ijA}(t);\ dP(t) = P^{in}_{ijA_{total}}(t) + \Delta P(t) - P^{dr}_{ijC_{total}}(t)$; Compute $P_{ijB}(t)$, using Eq. (3.10).
                    $P_{DG}(t) = 0$
                else

$P_{ijB}(t) = P^{dr}_{ijB}(t)$
if $(P_{DG_{rtd}} \geq P^{in}_{ijA_{total}}(t) - P^{dr}_{ijB_{total}}(t) + \Delta P(t) - P^{dr}_{ijC_{total}}(t))$ **then**
$P_{DG_e}(t) = P^{in}_{ijA_{total}}(t) - P^{dr}_{ijB_{total}}(t) + \Delta P(t) - P^{dr}_{ijC_{total}}(t)$
$P_{ijA}(t) = P^{in}_{ijA}(t);\ P_{DG}(t) = P_{DG_e}(t)$
else
$P_{DG}(t) = P_{DG_e}(t)P_{DG_{rtd}}(t);\ \ dP(t) = P^{dr}_{ijB_{total}}(t) - \Delta P(t) + P^{dr}_{ijC_{total}}(t) + P_{DG_e}(t)$; Compute $P_{ijA}(t)$, using Eq. (3.10).
end if
end if
end if
else
$P_{mg}(t) = \Delta P(t)$
if $(P^{in}_{ijA_{total}}(t) \leq P^{dr}_{ijC_{total}}(t) - \Delta P(t))$ **then**
$dP(t) = P^{in}_{ijA_{total}}(t) + \Delta P(t)$; Compute $P_{ijC}(t)$, using Eq. (3.10).
$P_{ijA}(t) = P^{in}_{ijA}(t);\ P_{ijB}(t) = 0; P_{DG}(t) = 0$
else
$P_{ijC}(t) = P^{dr}_{ijC}(t)$
if $(P^{in}_{ijA_{total}}(t) \leq P^{dr}_{ijB_{total}}(t) + P^{dr}_{ijC_{total}}(t) - \Delta P(t))$ **then**
$dP(t) = P^{in}_{ijA_{total}}(t) - P^{dr}_{ijC_{total}}(t) + \Delta P(t)$; Compute $P_{ijB}(t)$, using Eq. (3.10).
$P_{ijA}(t) = P^{in}_{ijA}(t);\ P_{DG}(t) = 0$
else
$P_{ijB}(t) = P^{dr}_{ijB}(t)$
if $(P_{DG_{rtd}} \geq P^{in}_{ijA_{total}}(t) - P^{dr}_{ijB_{total}}(t) - P^{dr}_{ijC_{total}}(t) + \Delta P(t))$ **then**
$P_{DG_e}(t) = P^{in}_{ijA_{total}}(t) - P^{dr}_{ijB_{total}}(t) - P^{dr}_{ijC_{total}}(t) + \Delta P(t)$
$P_{ijA}(t) = P^{in}_{ijA}(t);\ P_{DG}(t) = P_{DG_e}(t)$
else
$P_{DG}(t) = P_{DG_e}(t) = P_{DG_{rtd}}(t);\ dP(t) = P_{DG_e}(t) + P^{dr}_{ijB_{total}}(t) + P^{dr}_{ijC_{total}}(t) - \Delta P(t)$; Compute $P_{ijA}(t)$, using Eq. (3.10).
end if
end if
end if
end if
else if $(\Delta P(t) < 0)$ **then**
if $(P^{in}_{ijA_{total}}(t) \geq \Delta P(t))$ **then**
$P_{mg}(t) = \Delta P(t)$
if $(P^{in}_{ijA_{total}}(t) \geq \Delta P(t) + P^{dr}_{ijC_{total}}(t))$ **then**
$P_{ijC}(t) = P^{dr}_{ijC}(t)$
if $(P^{in}_{ijA_{total}}(t) \geq \Delta P(t) + P^{dr}_{ijC_{total}}(t) + P^{dr}_{ijB_{total}}(t))$ **then**
$P_{ijB}(t) = P^{dr}_{ijB}(t)$
if $(P_{DG_{rtd}} \geq P^{in}_{ijA_{total}}(t) - \Delta P(t) - P^{dr}_{ijC_{total}}(t) - P^{dr}_{ijB_{total}}(t))$ **then**

$P_{DG_e}(t) = P^{in}_{ijA_{total}}(t) - \Delta P(t) - P^{dr}_{ijC_{total}}(t) - P^{dr}_{ijB_{total}}(t)$
$P_{ijA}(t) = P^{in}_{ijA}(t);\ P_{DG}(t) = P_{DG_e}(t)$
else
$P_{DG}(t) = P_{DG_e}(t) = P_{DG_{rtd}}(t);\ dP(t) = P_{DG_e}(t) + \Delta P(t) + P^{dr}_{ijC_{total}}(t) + P^{dr}_{ijB_{total}}(t)$; Compute $P_{ijA}(t)$, using Eq. (3.10).
end if
else
$dP(t) = P^{in}_{ijA_{total}}(t) - \Delta P(t) - P^{dr}_{ijC_{total}}(t)$; Compute $P_{ijB}(t)$, using Eq. (3.10).
$P_{ijA}(t) = P^{dr}_{ijA}(t);\ P_{DG}(t) = 0$
end if
else
$dP(t) = P^{in}_{ijA_{total}}(t) - \Delta P(t)$; Compute $P_{ijC}(t)$, using Eq. (3.10).
$P_{ijA}(t) = P^{in}_{ijA}(t);\ P_{DG}(t) = 0;\ P_{ijB}(t) = 0$
end if
else
$P_{ijA}(t) = P^{in}_{ijA}(t);\ P_{ijC}(t) = 0;\ P_{ijB}(t) = 0;\ P_{DG}(t) = 0$
end if
else if $(\Delta P(t) = 0)$ **then**
$P_{mg}(t) = 0$
if $(P^{in}_{ijA_{total}}(t) \geq P^{dr}_{ijC_{total}}(t))$ **then**
$P_{ijC}(t) = P^{dr}_{ijC}(t)$
if $(P^{in}_{ijA_{total}}(t) \geq P^{dr}_{ijC_{total}}(t) + P^{dr}_{ijB_{total}}(t))$ **then**
$P_{ijB}(t) = P^{dr}_{ijB}(t)$
if $(P_{DG_{rtd}} \geq P^{in}_{ijA_{total}}(t) - P^{dr}_{ijC_{total}}(t) - P^{dr}_{ijB_{total}}(t))$ **then**
$P_{DG_e}(t) = P^{in}_{ijA_{total}}(t) - P^{dr}_{ijC_{total}}(t) - P^{dr}_{ijB_{total}}(t);\ P_{ijA}(t) = P^{in}_{ijA}(t);\ P_{DG}(t) = P_{DG_e}(t)$
else
$P_{DG}(t) = P_{DG_e}(t) = P_{DG_{rtd}}(t);\ dP(t) = P_{DG_e}(t) + P^{dr}_{ijC_{total}}(t) + P^{dr}_{ijB_{total}}(t)$; Compute $P_{ijA}(t)$, using Eq. (3.10).
end if
else
$dP(t) = P^{in}_{ijA_{total}}(t) - P^{dr}_{ijC_{total}}(t)$; Compute $P_{ijB}(t)$, using Eq. (3.10).
$P_{ijA}(t) = P^{dr}_{ijA}(t);\ P_{DG}(t) = 0$
end if
else
$dP(t) = P^{in}_{ijA_{total}}(t)$; Compute $P_{ijC}(t)$, using Eq. (3.10).
$P_{ijA}(t) = P^{in}_{ijA}(t);\ P_{DG}(t) = 0; P_{ijB}(t) = 0$
end if
end if
end for

Algorithm 2 is designed to provide an optimal schedule for DG unit and fleet of EVs at CS.

Primarily, different EVs at CS and their respective charging/discharging specifications provided by user are registered. The corresponding ΔP and voltage at microgrid bus are also registered in the controller. Afterwards, for each EV, $E_{ijk}(t)$ is computed followed by computation of corresponding $P_{ijk}^{in/dr}(t)$ and $C_{rate_{ijk}}(t)$.

$$C_{rate_{ijk}}(t) = \frac{P_{ijk}^{in/dr}(t)}{E_{ijk}(t)} \tag{3.9}$$

Algorithm 2 ensures that the $C_{rate_{ijk}}(t)$ calculated in Eq. (3.9) does not exceed EV owner's specified rate. If $C_{rate_{ijk}}(t)$ changes, $P_{ijk}^{in/dr}(t)$ is recalculated as illustrated in the algorithm. Subsequently, in accordance to the proposed control strategy, power is distributed among each EV as follows [37].

$$P_{ijk}(t) = \frac{P_{ijk}^{in/dr}(t)}{P_{ijk_{total}}^{in/dr}(t)} dP(t) \tag{3.10}$$

where, $dP(t)$ is the actual power to be distributed among EVs at CS. Further, if category C and dual mode EVs could not inject desired power into microgrid or EVs seeking charging, the controller switches on the DG unit. The suggested control efficiently enhances voltage profile of the system by injecting/drawing required power from microgrid. The magnitude of the microgrid bus voltage with implementation of proposed voltage controller is obtained from roots of following equation.

$$x^2 - V_r(t)x + R_0\Big\{\sum_{i=1}^{n(t)} P_i^{EV}(t) + P_{DG}(t)\Big\} = 0 \tag{3.11}$$

$$V_{min} \leq x \leq V_{max} \tag{3.12}$$

where, x represents the enhanced voltage at the microgrid bus, i.e., $V_s(t+\Delta t)$ and $V_r(t)$ is desired output voltage of the VSI at time t. $P_i^{EV}(t)$ is the sum of power distributed among all EVs present at CS at time t. Furthermore, the final SOC of EVs' batteries after charging/discharging at

time instant $(t+\Delta t)$ can be computed as follows.

$$SOC_{ijk}(t+\Delta t) = \frac{E^{st}_{ijk}(t) \pm [P_{ijk}(t) \times (t_{e_{ijk}} - t_{s_{ijk}})]}{E_{max_{ij}}} \times 100 \tag{3.13}$$

where, $SOC_{ijk}(t+\Delta t)$ represents the SOC of i^{th} EV of j^{th} type and k^{th} category after charging or discharging its battery at CS of the microgrid.

Chapter 4

RESULTS AND DISCUSSIONS

The efficacy of the developed voltage controller is validated through MATLAB programming. The ratings of the microgrid test system are listed in Table 4.1. The microgrid bus is considered to be having a nominal voltage and frequency of 400 V and 50 Hz respectively. The generation part consists of a 20 kW PV generation system and a 15 kW wind generation unit. The latter comprises of two wind turbines having rated capacity of 7.5 kW each. The variations in microgrids power generation and the demand profile across 24 hours is depicted in Fig. 4.1 and Fig. 4.2 respectively. The data for the solar, wind and load power curves is taken from [38] and scaled down to suit the assumed microgrid system. The peak load is assumed to be 35 kW. The microgrid bus voltage data for 24 hours is presumed on the basis of the net power obtained and is shown in Fig. 4.3.

Table 4.1: Ratings of Microgrid System

S.no.	Parameters	Values
1	Nominal voltage	400 V
2	Nominal frequency	50 Hz
3	Peak load	35 kW
4	Rated capacity of PV generation system	20 kW
5	Rated capacity of wind generation unit	(7.5*2) = 15 kW
6	Power rating of DG unit	35 kW

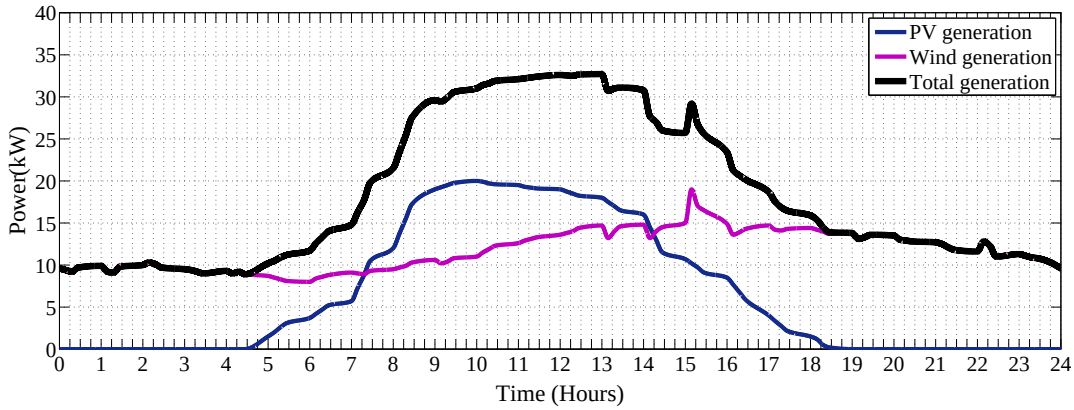

Figure 4.1: Power generation in the microgrid test system across 24 hours.

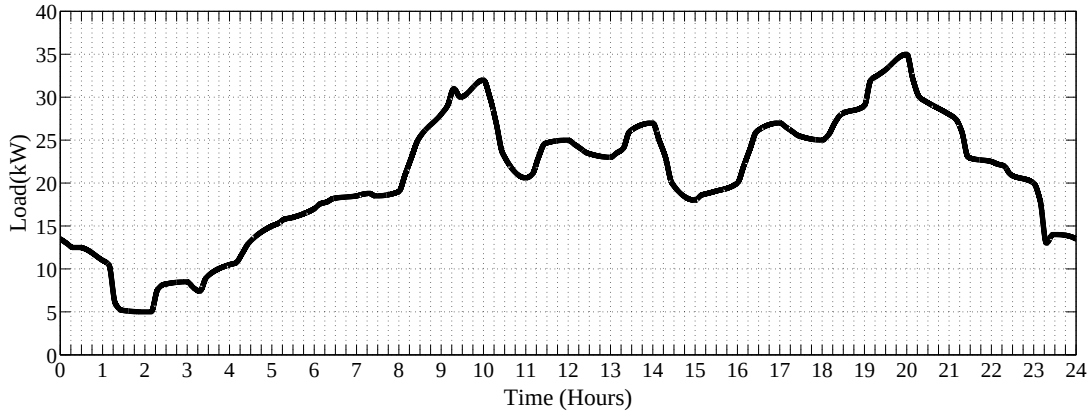

Figure 4.2: Load curve of microgrid test system.

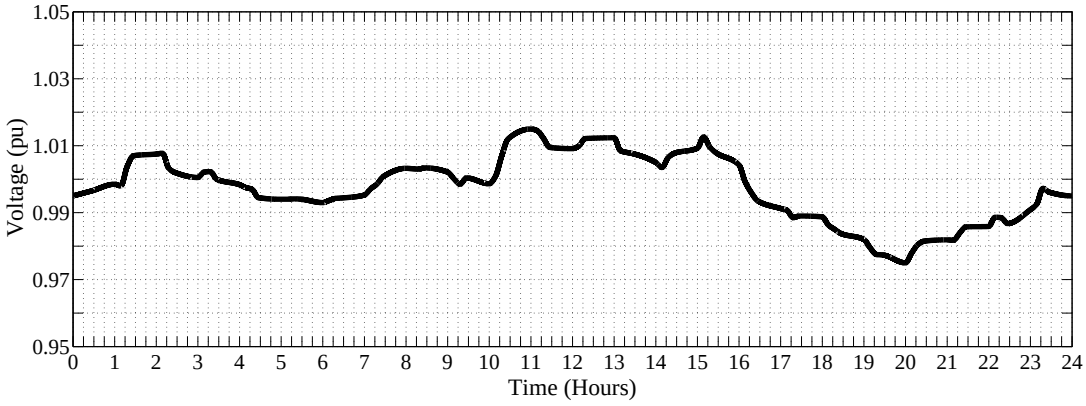

Figure 4.3: Bus voltage of the test microgrid system.

In order to mitigate voltage variations at the microgrid bus, the proposed voltage controller employs a P/V droop control unit and a PDCU. Fig. 4.4 shows P/V droop characteristics utilized in the control scheme. Based on these characteristics, the proposed controller provides the power ΔP to be injected or drawn from the microgrid at regular interval of 15 minutes, demonstrated in Fig. 4.5. ΔP is further distributed among EVs present at the CS through PDCU.

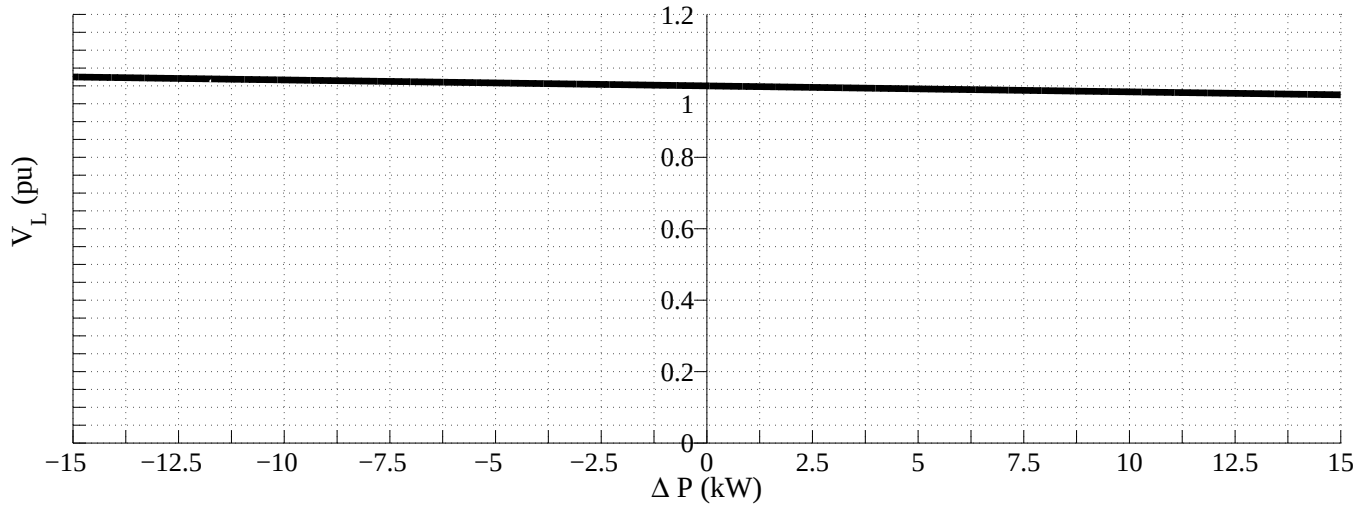

Figure 4.4: P/V droop characteristics employed in the proposed voltage control scheme.

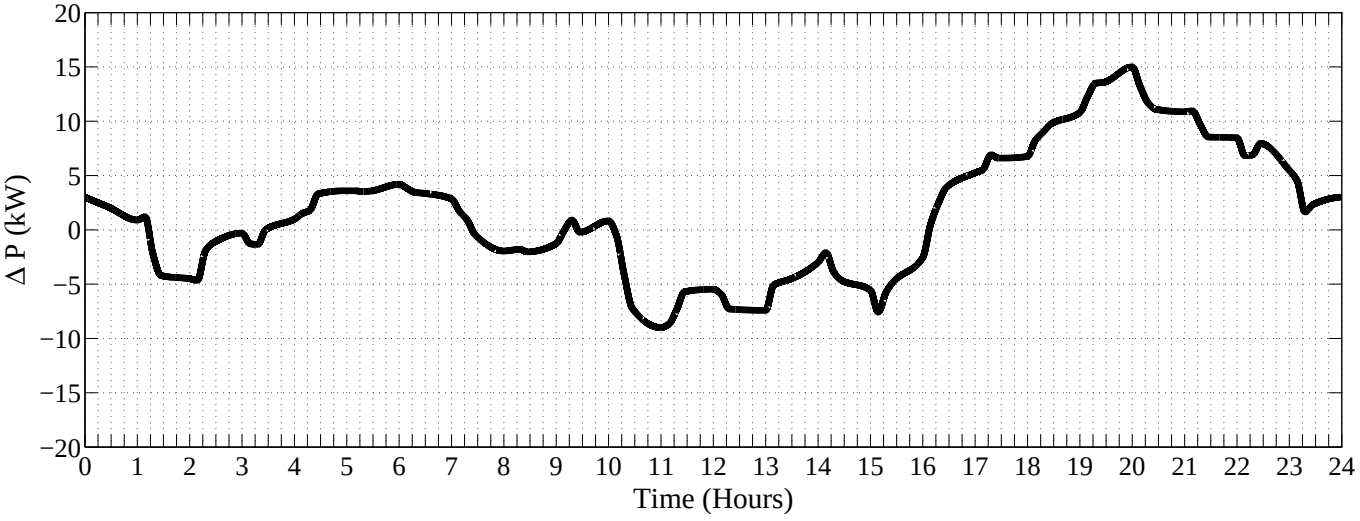

Figure 4.5: Power injected or drawn from microgrid as decided by the controller.

Three case studies are considered for different voltage conditions in the microgrid and corresponding scheduling of EVs is exemplified with simulation results. The objective of these case studies is to validate the efficacy of the developed control scheme in controlling voltage variations of system through active power compensation. In addition to it, the ability of suggested control in efficiently catering EVs' charging/discharging requests has also been verified. The simulation parameter for the proposed voltage controller are demonstrated in Table 4.2. The charging/discharging time of each EV is regulated through varying their C_{rate} by considering both microgrid's needs and time provided by respective owners.

Table 4.2: Simulation Parameters for P/V Droop Voltage Controller

S. no.	Parameters	Values
1	V_{ref}	1 p.u.
2	V_{max}	1.025 p.u.
3	V_{min}	0.975 p.u.
4	P_{ref}	20 kW
5	P_{max}	35 kW
6	P_{min}	5 kW
11	R	0.25 ohms

Case study I: In this case study, simulation is carried out for controller operation during voltage sag in the microgrid test system. As microgrid generation is less than the demand, controller outputs a positive ΔP. This further results in discharging of EVs present at the CS. During discharging of EVs, category C vehicles are given first priority to discharge their batteries. Further, if needed dual mode vehicles are discharged to supply the desired power in the test system.

Case study II: The simulations for voltage swell in the test system are carried out in this case study, when demand is more than the generation. Thus, controller results in a negative ΔP. The negative polarity of ΔP indicates need to draw power from the microgrid. This further results in charging of EVs at the CS. Category A vehicles are considered first for charging as they have their *SOC* below 40%.

Case study III: This case study considers the time interval when nominal voltage conditions prevail in the considered microgrid. During this case, no power flow occurs between microgrid and EVs. However, in order to fulfill charging/discharging needs of EVs present at the CS, power

exchange takes place between EVs in such a way that net power transfer is zero.

4.1 Case Study I: Voltage sag

This case study demonstrates decrease in microgrid voltage for duration of 7 hours i.e., 1700 hours - 2400 hours. Due to heavy loading and low power generation during this instant, the microgrid's voltage decreases from its nominal value (< 1 p.u.). The voltage difference ΔV is fed to the P/V droop control unit of the controller at regular interval of 15 minutes, which result in ΔP. This switches on PCS which in turn activates PDCU, thus initializing discharging of EVs at CS. Based upon user specified charging/discharging time, different categories of EVs available at the CS during the considered duration is illustrated in Fig. 4.6. Primarily, the current SOC and user specified charging/discharging requests is registered for all EVs. Based on this information, the controller computes the power that can be discharged or charged from the batteries of respective vehicles. In accordance to Algorithm 2, category C vehicles are discharged first during injecting power into microgrid. In this case study, the power offered to be discharged by category C EVs $P^{dr}_{ijC_{total}}$ as calculated by the controller and the corresponding ΔP is shown in Fig. 4.7. Further, depending upon the real time variations in EVs' SOC and charging/discharging requests, the controller operation will vary for each time interval, as demonstrated through following examples.

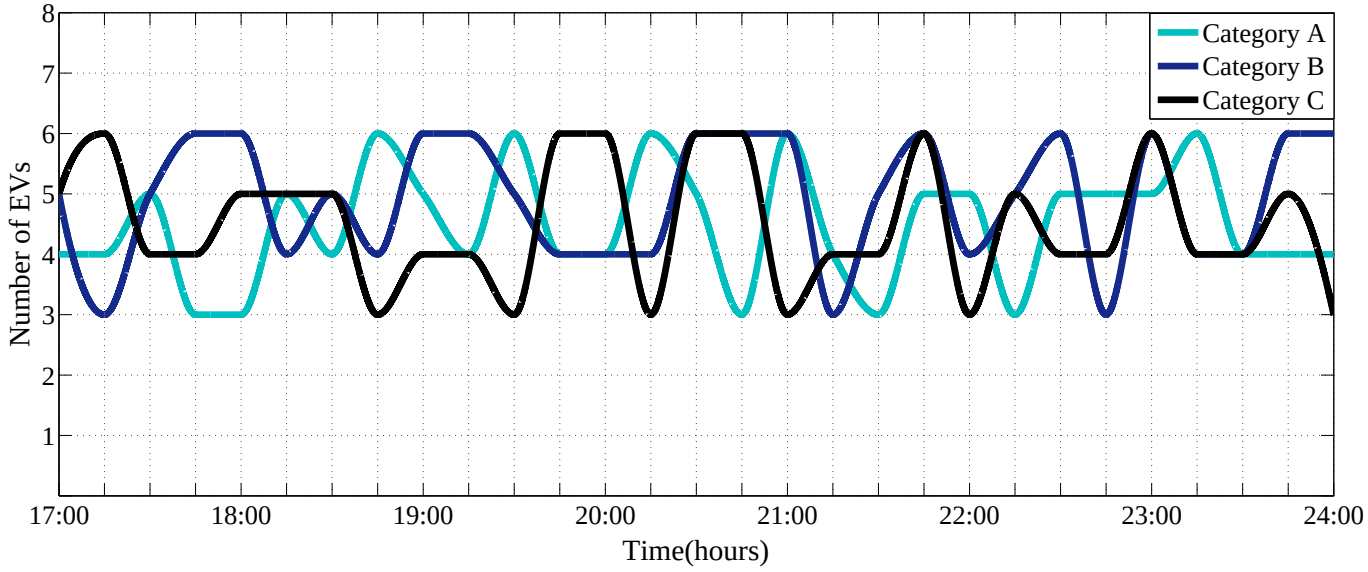

Figure 4.6: Different EVs present from 1700 hours - 2000 hours at the CS.

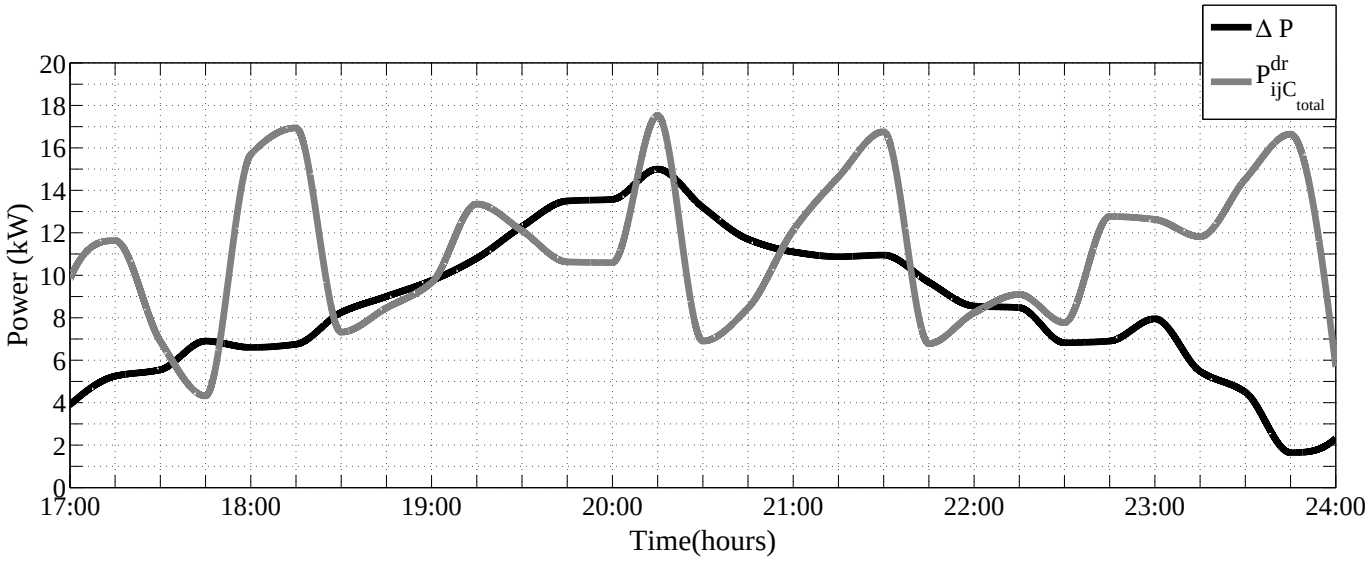

Figure 4.7: Power required by microgrid and offered by category C vehicles from 1700 hours - 2000 hours.

Example 1: This example considers voltage sag during time interval 2000 hours - 2015 hours. Various EVs present at the CS during this interval and their SOC are illustrated in Fig. 4.8. Six category C vehicles available at the CS offered $\{3.81\ 1.90\ 1.89\ 1.51\ 0.79\ 0.68\}$ kW power to discharge, which sums upto 10.58 kW. However, the corresponding ΔP is 13.57 kW as shown in Fig. 4.7. Thus, batteries of all 6 EVs are allowed to discharge the power offered by them. As power drawn from category C vehicles does not meet the test system's requirements, dual mode EVs are considered to supply the remaining 2.99 kW power. The power offered to discharge by category B vehicle owners is computed as $\{5.10\ 2.96\ 2.26\ 1.90\}$ kW. The total power that can be supplied by these vehicles is 12.22 kW, which is more than the microgrid's requirement. Thus, the surplus power is utilized for vehicles of category A present at CS for charging their batteries. Considering the charging needs of these EVs, power requested by corresponding EV owners is calculated and sorted as $\{15.05\ 11.29\ 10.54\ 4.65\}$ kW. Although, total power requested by EVs of category A is 41.53 kW, dual mode EVs supplies only 9.23 kW. As power provided by dual mode EVs is not sufficient to cater the power demanded by category A vehicles, the controller sends signal to switch on DG unit. Therefore, DG unit operates to supply remaining power i.e., 32.3 kW. This power is effectively distributed among category A vehicles by PDCU. During this interval, the power distributed among all EVs at CS is depicted in Fig. 4.9, where the positive and negative polarity of the power represents discharging and charging of EVs, respectively. The power division

amidst microgrid, EVs and DG unit is shown in Fig. 4.10.

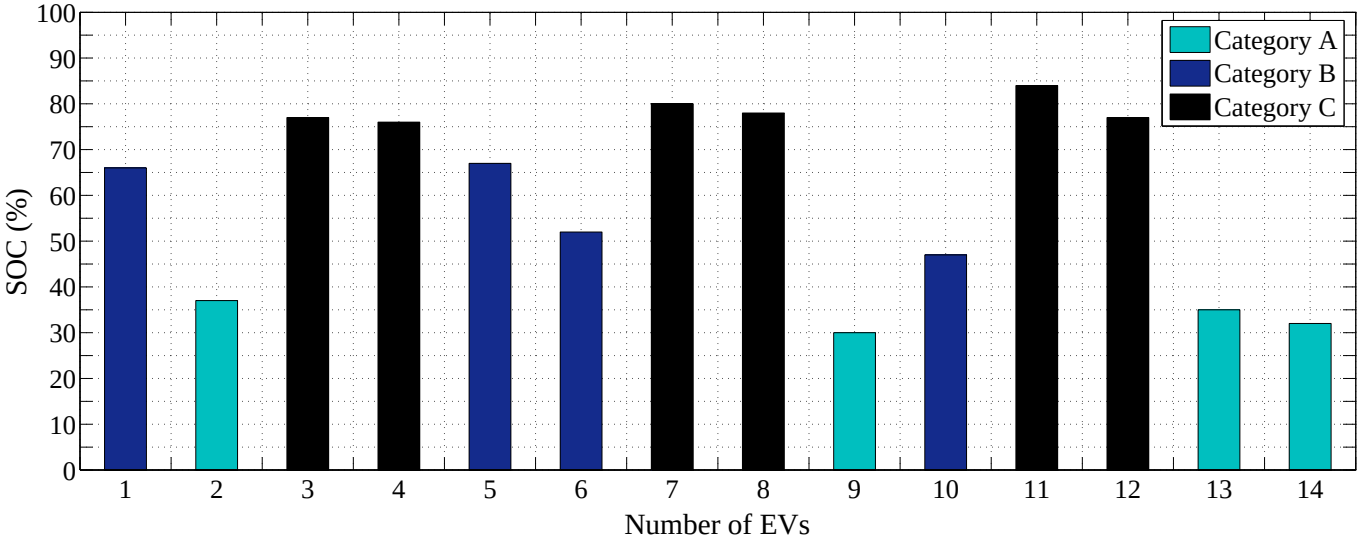

Figure 4.8: EVs present at the CS during time interval 2000 hours - 2015 hours.

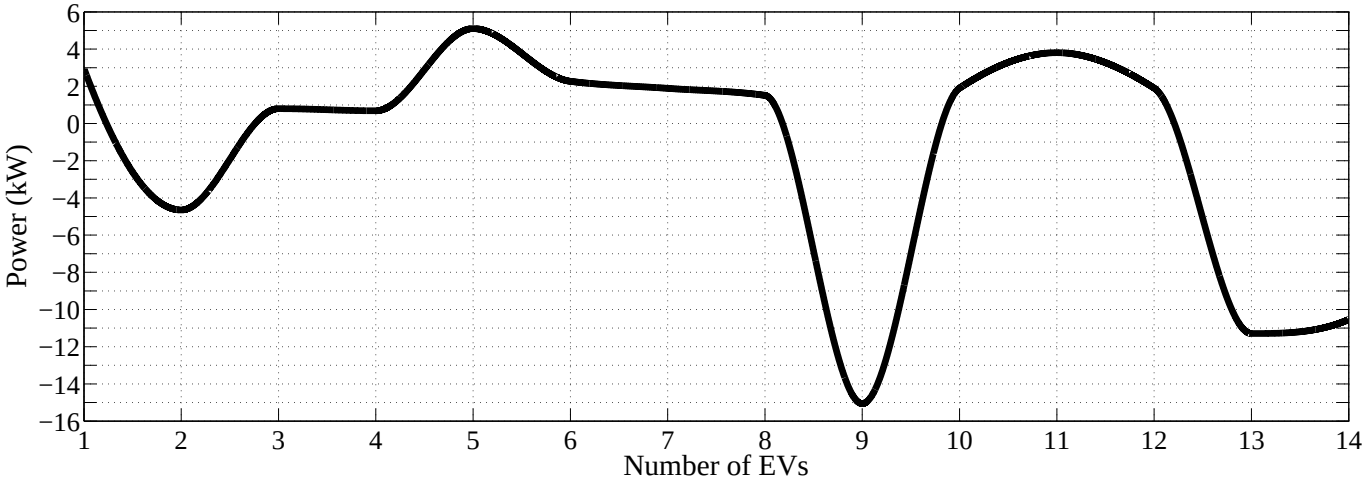

Figure 4.9: Power injected or drawn from EVs present at CS during 2000 hours - 2015 hours.

Example 2: The controller operation during time interval 2345 hours to 2400 hours is investigated in this example. Fifteen EVs of different categories are available at the CS during this time interval. Although similar to example 1, voltage sag conditions are examined but ΔP is less than the power offered to discharge by category C vehicles. Here, the power that can be drawn from batteries of category C vehicles is computed as $\{5.98\ 3.53\ 3.02\ 2.28\ 1.82\}$ kW, which sums up to 16.63 kW. However, ΔP i.e., the power needed to be injected into the microgrid is only 1.65

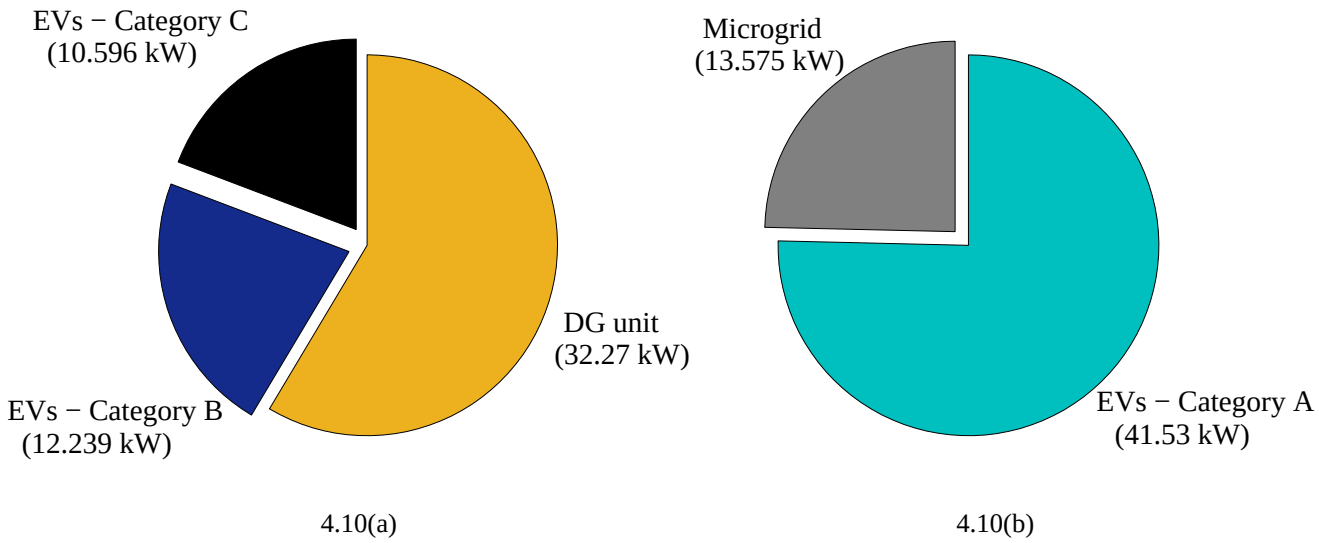

Figure 4.10: Power division among (a) DG unit, category C and category B vehicles for discharging purpose; (b) microgrid and category A vehicles seeking charging.

kW. Thus, after catering microgrid's requirement, remaining 14.98 kW power is utilized to charge category A vehicles having SOC below 40%. According to specifications provided by respective EV users, corresponding power needed for charging is calculated as $\{4.20\ 4.04\ 2.27\ 1.89\}$ kW. PDCU optimally divides power available from category C vehicles among EVs seeking charging. To ensure an optimal distribution of power, each EV shares power proportional to corresponding power offered. In this case, 5.05 kW and 1.53 kW power is drawn from EVs offering 5.98 kW and 1.82 kW, respectively. The power distribution among each EV at CS during the considered interval is elaborated in Fig. 4.11. It is evident from the figure that category C vehicles are capable of supplying power for desired voltage regulation at microgrid bus and charging category A vehicles. As a result, no power exchange takes place through dual mode EVs and DG unit remains switched off during this interval. Further, the SOC of EVs before and after charging/discharging is depicted in Fig. 4.12.

4.2 Case Study II: Voltage swell

This segment investigates voltage swell during time interval 1115 hours - 1615 hours, i.e., for a duration of 5 hours. Due to light loading at this instance, microgrids bus voltage V_s increases from

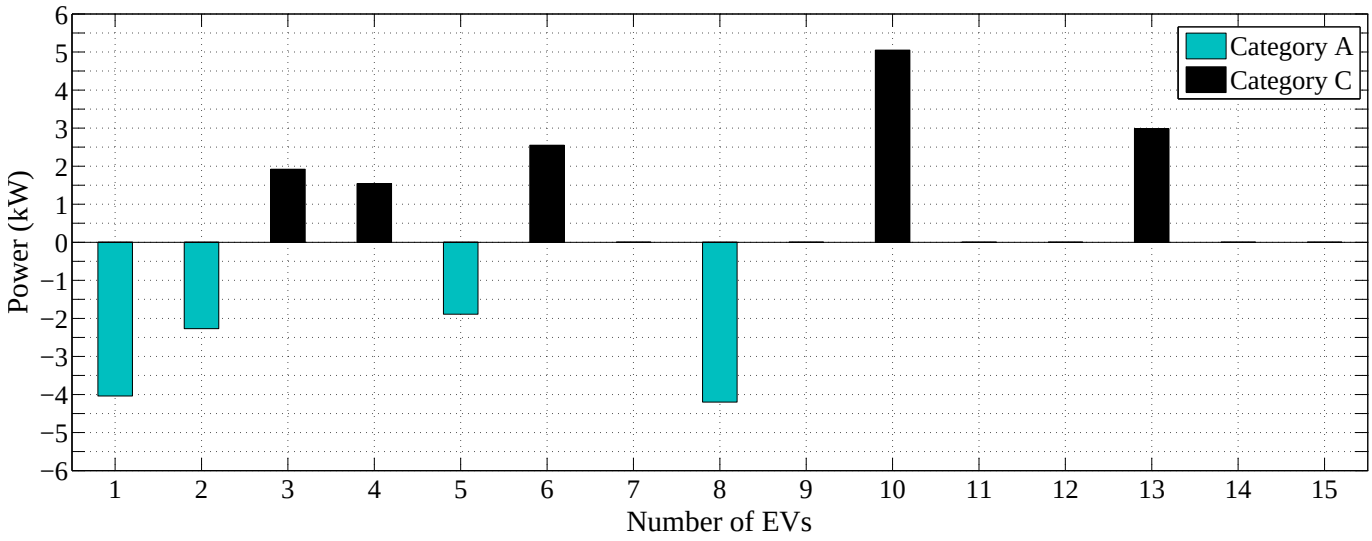

Figure 4.11: Power division among category A and category C vehicles during 2345 hours - 2400 hours.

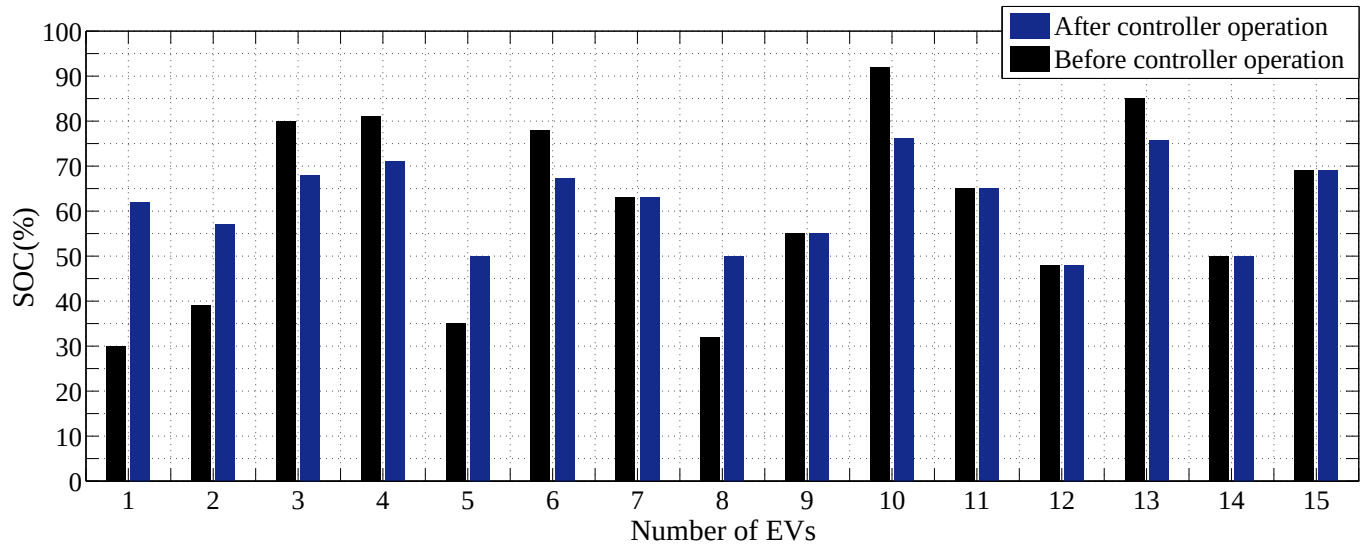

Figure 4.12: SOC of EVs at CS before and after charging/discharging during 2345 hours - 2400 hours.

its nominal value ($>$ 1 p.u.). At regular interval of 15 minutes, V_s is fed to the proposed controller. This voltage is then compared with V_{ref} to give ΔV, thus, activating P/V droop control unit. This results in negative ΔP, which is distributed among EVs seeking charging at the CS of the test system. Based on the initial SOC, different categories of EVs present at the CS during the considered interval is shown in Fig. 4.13. As explained earlier, first priority for charging is given to category A vehicles whenever power is drawn from microgrids. The power $P^{in}_{ijA_{total}}$, requested by category

A vehicle to charge their batteries and the magnitude of corresponding ΔP is shown in Fig. 4.14. Further, the controller operation during voltage swell in the test system is exemplified as follows.

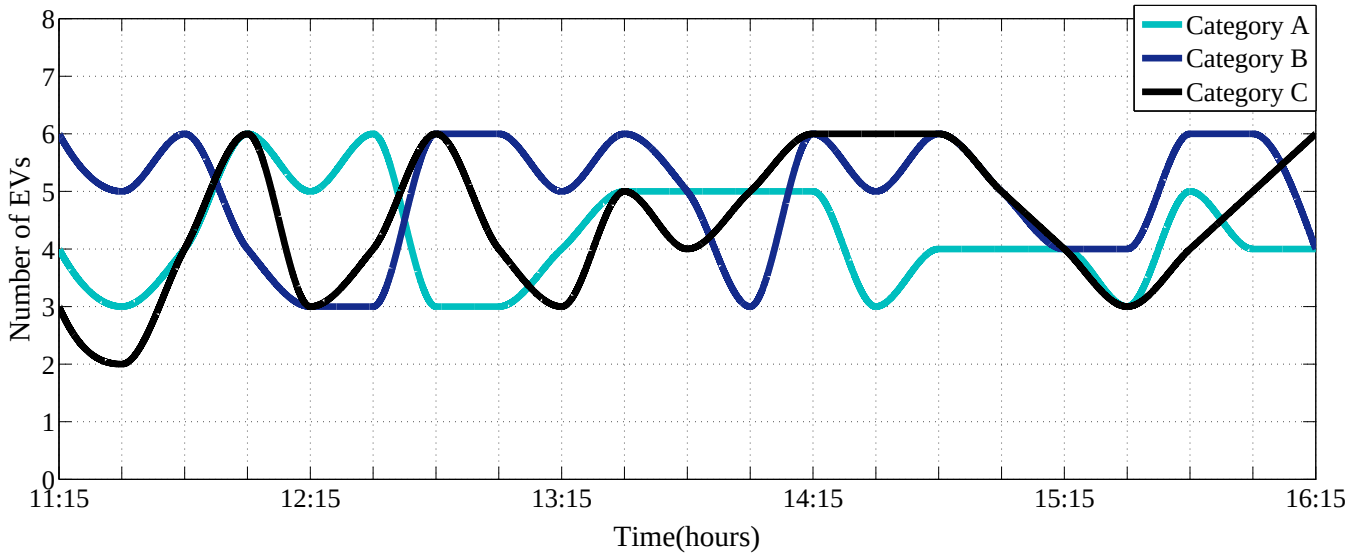

Figure 4.13: EVs at CS during 1115 hours - 1615 hours.

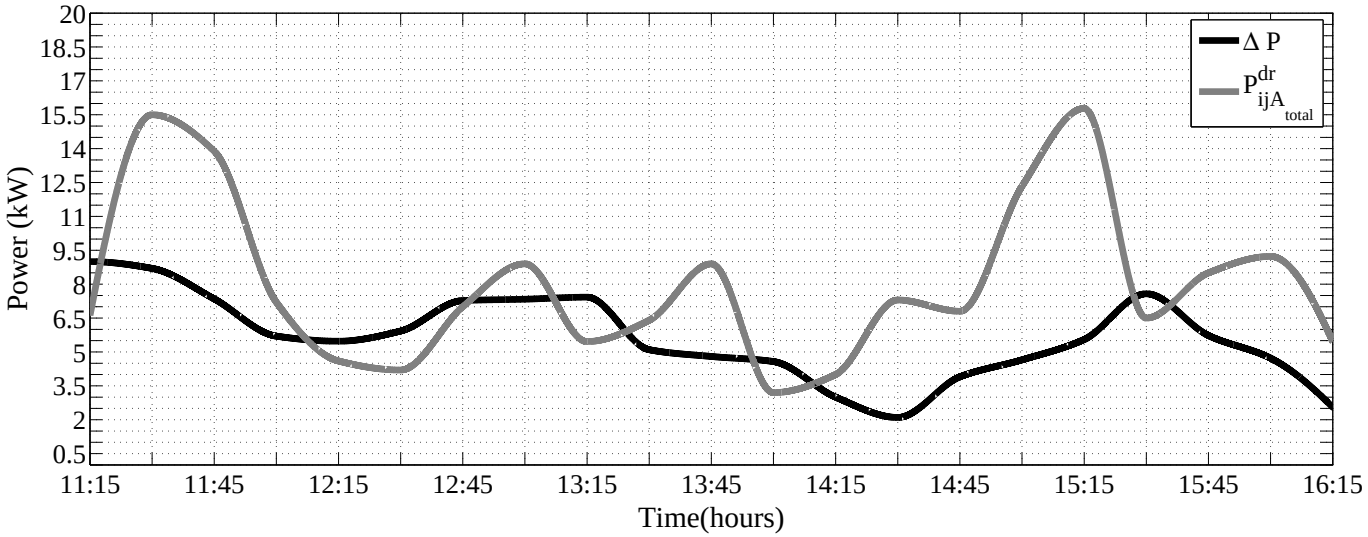

Figure 4.14: Power drawn from microgrid and requested by category A vehicles during 1115 hours - 1615 hours.

Example 3: This part analyses the increase in microgrid's bus voltage during time interval 1130 hours - 1145 hours, as total generation of the microgrid is greater than the demand. Thus, to restore the nominal voltage at the microgrid bus, the excess power is injected into the EVs. Types of 10 EVs present at CS during interval 1130 hours - 1145 hours and their respective SOC is shown in Fig. 4.15. As category A vehicles are having least SOC of all the categories, they

are charged first. Based on current and desired SOC of 3 EVs belonging to category A along with their respective user specified C_{rate}^{max} and SOC_{min}, the power requested by EV owners is computed and sorted as $\{7.93\ 4.04\ 3.53\}$ kW. Subsequently, the power to be drawn from microgrid i.e., ΔP is divided optimally among each EV considering their respective power demands as $\{4.45\ 2.26\ 1.98\}$ kW. The total power requested by EVs seeking charging at CS is 15.5 kW, which is more than ΔP. After distributing ΔP among category A vehicles, their power requests are updated as $\{3.48\ 1.78\ 1.55\}$ kW, which sums up to 6.8 kW. To supply the remaining 6.8 kW power, the controller will consider category C vehicles for discharging. The power offered by category C vehicles is computed considering their discharging requests as $\{9.52\ 3.21\}$ kW. In accordance to Algorithm 2, 6.8 kW power is divided optimally among these two EVs, such that the one offering more power is discharged more. In this case, 5.08 kW and 1.71 kW is drawn from EV offering 9.52 kW and 3.21 kW, respectively. The power distributed among all 10 EVs available during interval 1130 hours - 1145 hours is illustrated in Fig. 4.16. As power requested by category A vehicles is wholly supplied by EVs present at CS under category C, dual mode vehicles are neither charged nor discharged. DG unit will also remain switched off during this instant. Further, the charging and discharging of vehicles involved during this interval with their final SOC is depicted in 4.17.

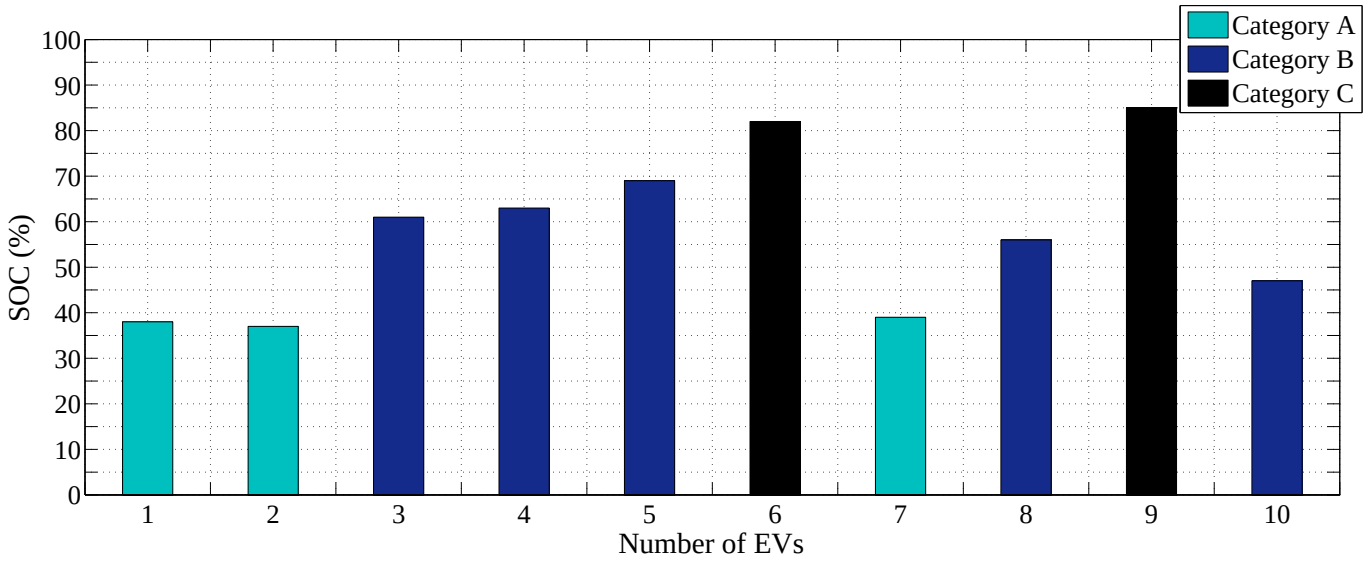

Figure 4.15: Different EVs present at CS from 1130 hours - 1145 hours.

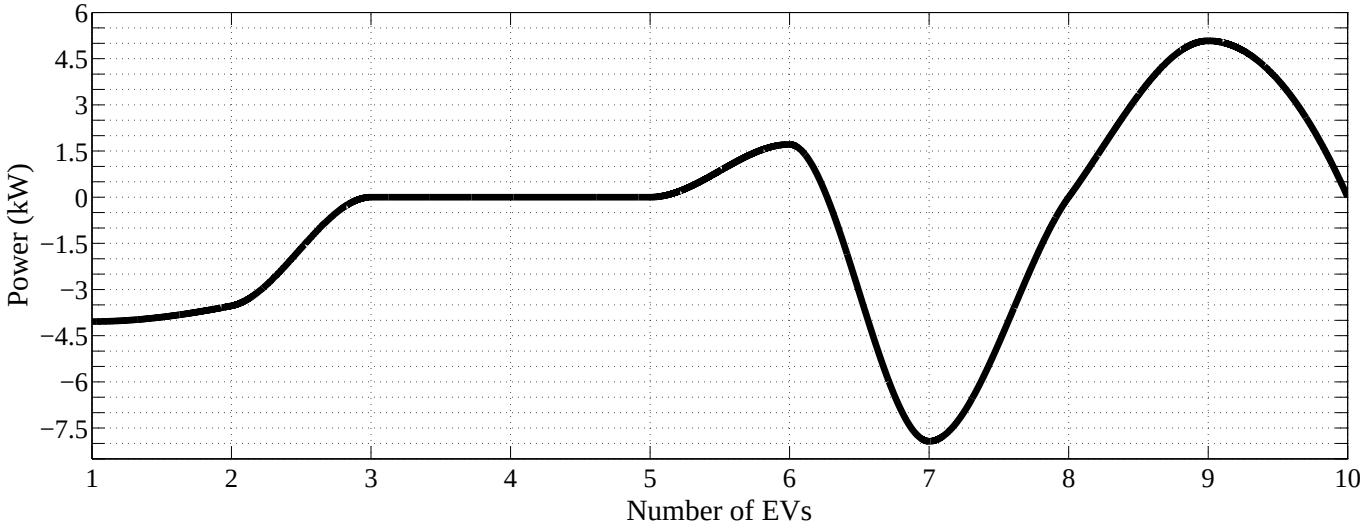

Figure 4.16: Power distribution among EVs at CS from 1130 hours - 1145 hours.

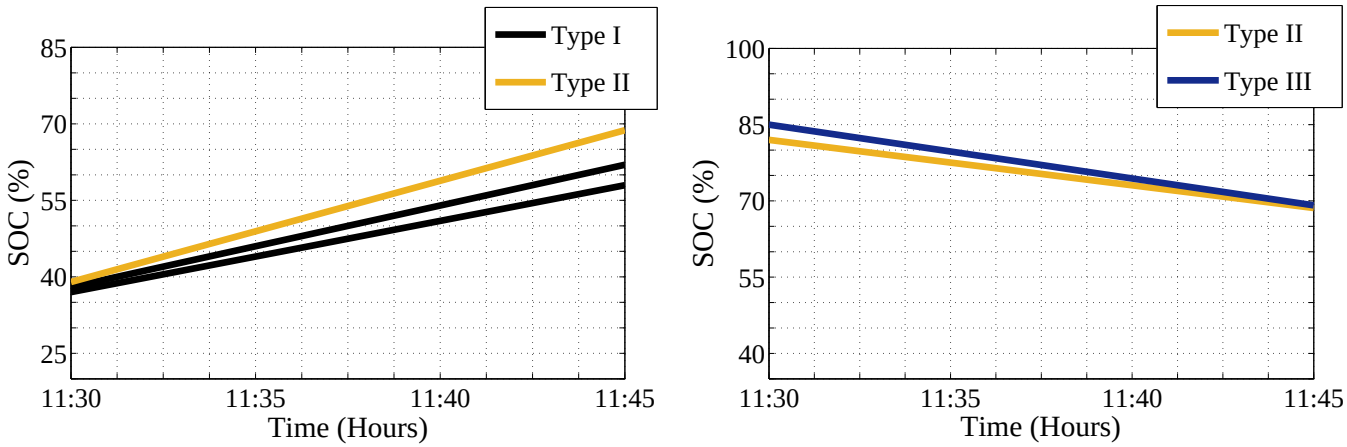

4.17(a) 4.17(b)

Figure 4.17: (a) Charging of category A vehicles at 1130 hours. (b) Discharging of category C vehicles at 1130 hours.

4.3 Case Study III: Nominal voltage

This case study sheds light on the controller's operation when nominal voltage conditions i.e. $(V_s = 1p.u.)$, prevails in the test system during 0400 hours - 0415 hours. ΔV is zero during this instant resulting in zero ΔP, thus, no power flows between microgrid and CS. However, EVs present at CS demand for charging and discharging of their batteries. Thus power flow occurs among EVs in such a way that net power flow between them is zero. Types and categories with SOC of 18 EVs available at CS are shown in Fig. 4.18. Considering user provided charging specifications the

controller determines power requested by category A EVs as {8.28 8.16 6.76 5.68 4.89} kW for charging their batteries. During this instance, the power offered by category C vehicles is computed as {10.06 4.78 4.34 1.93 1.71} kW. This power is distributed among category A vehicles by PDCU as {5.59 5.51 4.57 3.84 3.30}. However, this power is less than the power requested by the EVs. This leads to consideration of dual mode EVs for discharging their batteries. The power that can be discharged from category B EVs is {5.98 3.80 3.53 2.26 2.16 2.07 1.70 1.48} kW, which is sufficient to cater the charging needs of category A EVs. Finally utilizing Algorithm 2, the controller allocates power to category B EVs as {2.84 1.80 1.68 1.07 1.03 0.98 0.76 0.7} kW. The power distribution among all EVs present at CS during the considered interval is demonstrated in Fig.4.19. The DG unit will remain switched off during this case.

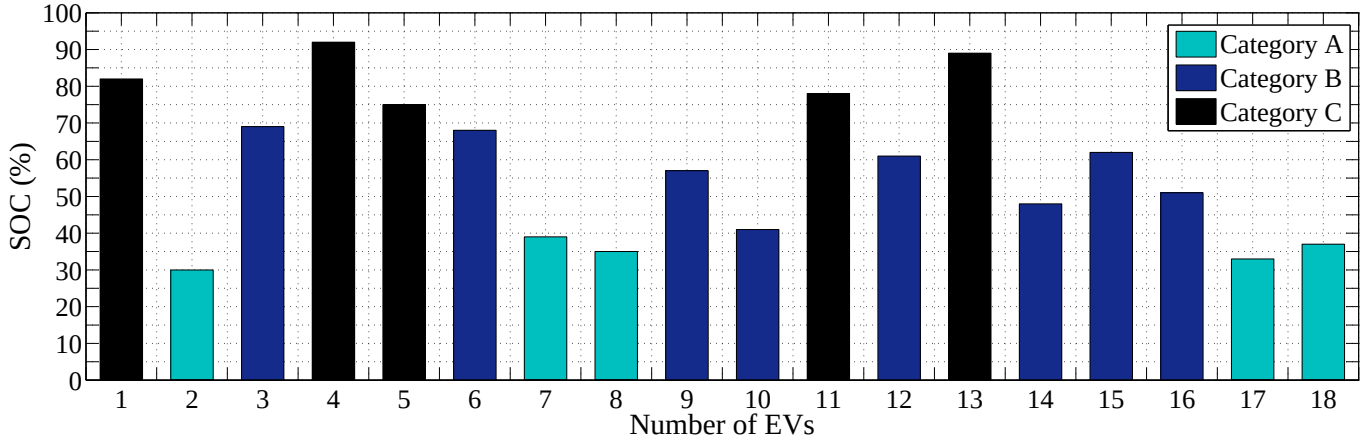

Figure 4.18: EVs at CS during 0400 hours - 0415 hours.

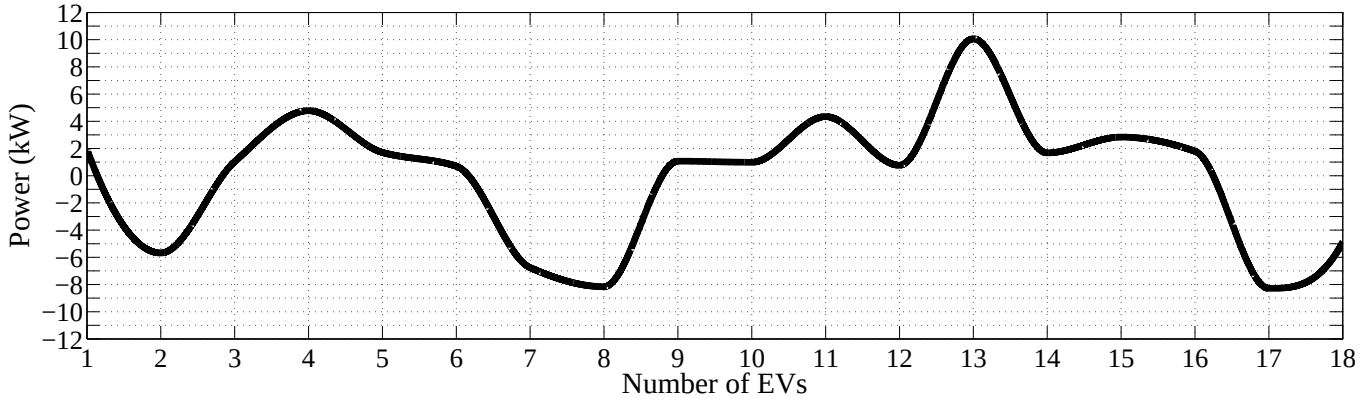

Figure 4.19: Power injected or drawn from EVs during 0400 hours - 0415 hours.

It can be concluded from above results that the proposed controller utilizes EVs efficiently, to

obtain peak shaving and valley filling, during peak and off peak hours respectively. This provides desired voltage regulations in microgrid test system. The voltage of the microgrid with and without P/V droop voltage controller is represented in Fig. 4.20. It can be observed that the voltage at microgrid bus is effectively maintained near unity by optimal charging/discharging of the EVs at CS.

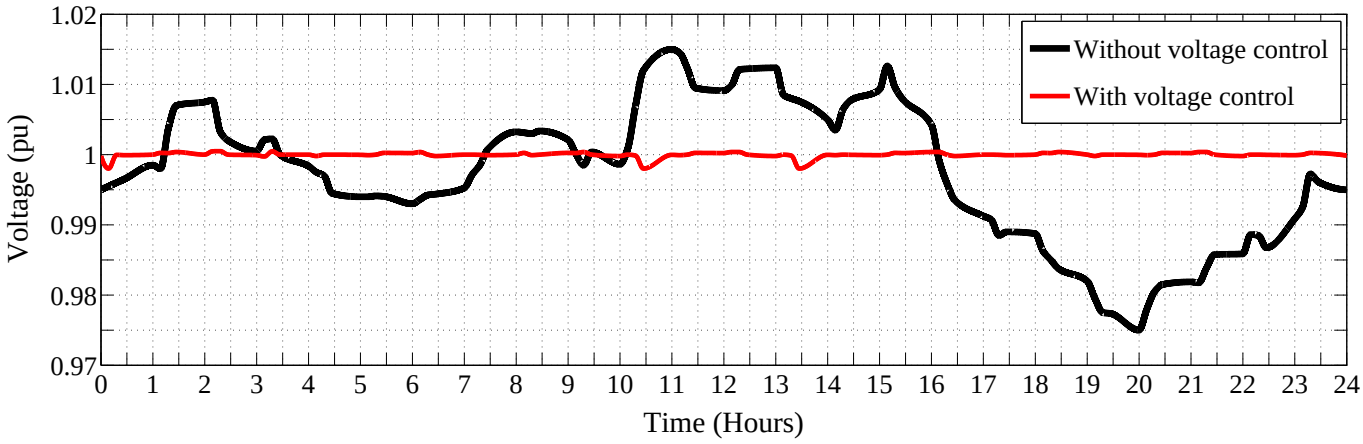

Figure 4.20: Microgrid bus voltage with and without votage control

Chapter 5

CONCLUSION AND FUTURE WORK

The integration of intermittent RESs in an LV islanded microgrid with fluctuating load may result in voltage variations. To resolve this issue, an islanded microgrid equipped with EVs for energy storage as well as voltage support is considered in this work. Further, a voltage controller is proposed to provide adequate voltage regulations at the test microgrid's bus. The suggested controller employs P/V droop characteristics to regulate active power flow between EVs and microgrid. The controller ensures optimal utilization of EVs as distributed energy source and ESS, to provide peak shaving and valley filling respectively, thus facilitating voltage regulation in the microgrid. Moreover, charging/discharging needs of EVs are fulfilled with respect to SOC limits and maximum charging rate. It is validated that controlling charging or discharging of EVs at CS can efficiently maintain microgrid's voltage close to specified nominal voltage.

The future work will include application of the proposed controller in a microgrid integrated with more than one CS. The efficacy of the suggested scheme will be observed with respect to coordination among multi-charging stations and EVs. In addition to it, a modified voltage controller will be developed for fulfilling the EVs' owners requirements more efficiently and reliably.

LIST OF PUBLICATIONS

1. S. Jagota, M. Singh and S. Singh, "A Novel Droop Based Voltage Control using EV Charging Station in an Islanded Microgrid," *IEEE Transactions on Sustainable Energy*. (manuscript under preparation)

BIBLIOGRAPHY

[1] G. Venkataramanan and C. Marnay, "A larger role for microgrids," *IEEE Power and Energy Magazine*, vol. 6, no. 3, pp. 78-82, May 2008.

[2] R. Chowdhury and T. Boruah, "Design of a micro-grid system in matlab/simulink," *International Journal of Innovative Research in Science, Engineering & Technology*, vol. 4, issue 7, pp. 5262-5269, July 2015.

[3] A. Banerji, D. Sen, A. K. Bera, D. Ray, D. Paul, A. Bhakat and S. K. Biswas, "Microgrid: A review," *in Proc. IEEE Global Humanitarian Technology Conference: South Asia Satellite*, Aug. 2013, pp. 27-35.

[4] R. H. Lasseter, "MicroGrids," *IEEE PES Winter Meeting*, vol. 1, Jan. 2002, pp. 305-308.

[5] B. S. Hartono, Y. Budiyanto and R. Setiabudy, "Review of microgrid technology," *in Proc. IEEE International Conference on Quality in Research*, Jun. 2013, pp. 127-132.

[6] X. Liu and B. Su, "Microgrids - An integration of renewable energy technologies," *in Proc. IEEE China International Conference on Electricity Distribution*, Dec. 2008, pp. 1-7.

[7] A. Ravichandran, P. Malysz, S. Sirouspour and A. Emadi, "The critical role of microgrids in transition to a smarter grid: a technical review," *in Proc. IEEE Transportation Electrification Conference & Expo*, Jun. 2013, pp. 1-7.

[8] R. H. Lasseter and P. Paigi, "Microgrid: a conceptual solution," *in Proc. IEEE* 35^{th} *Power Electronic Specialist Conference*, vol. 6, Jun. 2004, pp. 4285-4290.

[9] D. E. Olivares, A. Mehrizi-Sani, *et al.*, "Trends in microgrid control," *IEEE Transactions on Smart Grid*, vol. 5, no. 4, pp. 1905-1919, July 2014.

[10] R. Shigenobu and T. Funabashi, "Multi-objective optimization of SVR considering optimum placement and weather conditions in distribution systems," *in Proc. IEEE* 18^{th} *International Conference on Intelligent System Application to Power Systems*, Sep. 2015, pp. 1-6.

[11] R. H. Lasseter, A. Akhil, C. Marnay, J. Stevens, J. Dagle, R. Guttromson, A. S. Meliopoulous, R. Yinger and J. Eto, White Paper on Integration of Distributed Energy Resources—The CERTS MicroGrid Concept. [Online]. Available: https://certs.lbl.gov/sites/all/files/lbnl-50829.pdf.

[12] X. Chen, Y. Hou, S.C. Tan, C. K. Lee and S.Y. R. Hui, "Mitigating voltage and frequency fluctuation in microgrids using electric springs," *IEEE Transactions on Smart Grid*, vol. 6, no. 2, pp. 508-515, Mar. 2015.

[13] R. Majumder, "Reactive power compensation in single-phase operation of microgrid," *IEEE Transactions on Industrial Electronics*, vol. 60, no. 4, pp. 1403-1416, Apr. 2013.

[14] T. L. Lee, S. H. Hu and Y. H. Chan, "D-STATCOM with positive-sequence admittance and negative-sequence conductance to mitigate voltage fluctuations in high-level penetration of distributed-generation systems," *IEEE Transactions on Industrial Electronics*, vol. 60, no. 4, pp. 1417-1428, Apr. 2013.

[15] B. W. Frana, L. F. da Silva, M.A. Aredes and M. Aredes, "An improved iUPQC controller to provide additional grid-voltage regulation as a STATCOM," *IEEE Transactions on Industrial Electronics*, vol. 62, no. 3, pp. 1345-1352, Mar. 2015.

[16] X. Huang, X. Jin, T. Ma and Y. Tong, "A voltage and frequency droop control method for microsources," *in Proc. IEEE International Conference on Electrical Machines and Systems*, Aug. 2011, pp. 1-5.

[17] J. A. Pecas Lopes and C. L. Moreira, "Defining control strategies for microgrids islanded operation," *IEEE Transactions on Power Systems*, vol. 21, no. 2, pp. 916-924, May 2006.

[18] C. K. Sao and P. W. Lehn, "Control and power management of converter fed microgrids," *IEEE Transactions on Power Systems*, vol. 23, no. 3, pp. 1088-1098, Aug. 2008.

[19] P. Chaweewat, J. G. Singh, W. Ongsakul and A. K. Srivastava, "Synchronization control and droop control of microgrid operation," *in Proc. IEEE International Conference and Utility Exhibition on Green Energy for Sustainable Development*, Mar. 2014, pp. 1-7.

[20] Z. Ziadi, S. Taira, M. Oshiro and T. Funabashi, "Optimal power scheduling for smart grids considering controllable loads and high penetration of photovoltaic generation," *IEEE Transactions on Smart Grid*, vol. 5, no. 5, pp. 2350-2359, Sep. 2014.

[21] T. Morstyn, B. Hredzak and V. G. Agelidis, "Distributed cooperative control of microgrid storage," *IEEE Transactions on Power Systems*, vol. 30, no. 5, pp. 2780-2789, Sep. 2015.

[22] J. Y. Kim, J. H. Jeon, S. K. Kim, C. Cho, J. H. Park, H. M. Kim and K. Y. Nam, "Cooperative control strategy of energy storage System and microsources for stabilizing the microgrid during islanded operation," *IEEE Transactions on Power Electronics*, vol. 25, no. 12, pp. 3037-3048, Dec. 2010.

[23] M. Falahi, H. M. Chou, M. Ehsani, L. Xie and K. L. Butler-Purry, "Potential power quality benefits of electric vehicles," *IEEE Transactions on Sustainable Energy*, vol. 4, no. 4, pp. 1016-1023, Oct. 2013.

[24] P. Mitra, G. K. Venayagamoorthy and K. A. Corzine, "SmartPark as a virtual STATCOM," *IEEE Transactions on Smart Grid*, vol. 2, no. 3, pp. 445-455, Sep. 2011.

[25] W. Yao, M. Chen, J. Matas, J. M. Guerrero and Z. M. Qian, "Design and analysis of the droop control method for parallel inverters considering the impact of the complex impedance on the power sharing," *IEEE Transactions on Industrial Electronics*, vol. 58, no. 2, pp. 576-588, Feb. 2011.

[26] H. Laaksonen, P. Saari and R. Komulainen, "Voltage and frequency control of inverter based weak LV network microgrid," *in Proc. IEEE International Conference on Future Power Systems*, Nov. 2005, pp. 1-6.

[27] X. Chen, W. Shen, T. T. Vo, Z. Cao and A. Kapoor, "An overview of lithium-ion batteries for electric vehicles ," *in Proc. IEEE Conference on Power and Energy*, Dec. 2012, pp. 230-235.

[28] F. Nemry, G. Leduc, and A. Muoz, Plug-in hybrid and battery-electric vehicles: State of the research and development and comparative analysis of energy and cost efficiency, JRC Technical Notes, 2009 [Online]. Available: http://ftp.jrc.es/EURdoc/JRC54699_TN.pdf

[29] K. Zou, A. P. Agalgaonkar, K. M. Muttaqi, S. Perera and N. Browne, "Support of distribution system using distributed wind and PV systems," *in Proc. IEEE Australasian Universities Power Engineering Conference*, Sep. 2009, pp. 1-6.

[30] R. Karki, P. Hu and R. Billinton, "A simplified wind power generation model for reliability evaluation," *IEEE Transactions on Energy Conversion*, vol. 21, no. 2, pp. 533-540, Jun. 2006.

[31] W. L. Hsieh, C. H. Lin, C. S. Chen, C.T. Hsu, T. T. Ku, C. T. Tsai and C. Y. Ho, "Impact of PV generation to voltage variation and power losses of distribution systems," *in Proc. IEEE* 4^{th} *International Conference on Electric Utility Deregulation and Restructuring and Power Technologies*, July 2011, pp. 1474-1478.

[32] P. Giorsetto and K. F. Utsurogi, "Development of a new procedure for reliability modeling of wind turbine generators," *IEEE Transactions on Power Apparatus and Systems*, vol. PAS-102, no. 1, pp. 134-143, Jan. 1983.

[33] P. H. Huang and T. H. Tseng, "Analysis for effects of load characteristics on power system voltage stability," *in Proc. AASRI Conference on Power and Energy Systems*, Dec. 2012, pp. 229-234.

[34] A. B. Almeida, E. V. D. Lorenci, R. C. Leme, A. C. Z. D. Souza, B. I. L. Lopes and K. Lo, "Probabilistic voltage stability assessment considering renewable sources with the help of the PV and QV curves," *IET Renewable Power Generation*, vol. 7, no. 5, pp. 521-530, Sep. 2013.

[35] Y. A. Jabri, N. Hosseinzadeh, R. A. Abri and A. A. Hinai, "Voltage stability assessment of a microgrid," *in Proc. IEEE* $8^{t}h$ *GCC Conference and Exhibition*, Feb. 2015, pp. 1-6.

[36] L. M. Vargas, J. Jatskevich and J. R. Mart, "Induction motor loads and voltage stability assessment using PV curves," *IEEE PES General Meeting*, July 2009, pp. 1-7.

[37] M. Singh, P. Kumar and I. Kar, "A multi charging station for electric vehicles and its utilization for load management and the grid support," *IEEE Transactions on Smart Grid*, vol. 4, no. 2, pp. 1026-1037, Jun. 2013.

[38] M. George and R. Banerjee, "A methodology for analysis of impacts of grid integration of renewable energy," *Energy Policy*, vol. 39, no. 3, pp. 1265-1276, Mar. 2011 .

CURRICULUM VITAE OF AUTHOR

I. Introduction

NAME	**:**	Shubhangi Jagota
FATHER'S NAME	**:**	Er. Vijay Jagota
DATE OF BIRTH	**:**	02/03/1993
E-mail	**:**	shubhangi.jagota@gmail.com

II. Educational Qualification

Examination	**Institute**	**Board/University**	**Marks(% or CGPA)**
AISSCE	D.A.V Public School	C.B.S.E	66.8
AISSE	D.A.V Public School	C.B.S.E	79.6
B.Tech - Electrical and Electronics Engg.	Amritsar College of Engg. and Technology	Punjab Technical University	69.68
M.E.- Power Systems	Thapar Institute of Engg. and Technology	T.I.E.T University	8.49*

Shubhangi

ORIGINALITY REPORT

3%	2%	2%	0%
SIMILARITY INDEX	INTERNET SOURCES	PUBLICATIONS	STUDENT PAPERS

PRIMARY SOURCES

1	Yang Han, Pan Shen, Ernane Coelho, Josep Guerrero. "Review of Active and Reactive Power Sharing Strategies in Hierarchical Controlled Microgrids", IEEE Transactions on Power Electronics, 2016 Publication	<1%
2	Buque, C., O. Ipinnimo, S. Chowdhury, and S. P. Chowdhury. "Modeling and simulation of an Adaptive Relaying Scheme for a Microgrid", 2012 IEEE Power and Energy Society General Meeting, 2012. Publication	<1%
3	www.mdpi.com Internet Source	<1%
4	edoc.ub.uni-muenchen.de Internet Source	<1%
5	Submitted to Amrita Vishwa Vidyapeetham Student Paper	<1%
6	ethesis.nitrkl.ac.in Internet Source	<1%

7	R.A. Dougal. "Virtual-prototyping satellite electrical power systems using the virtual test bed", Proceedings IEEE SoutheastCon 2002 (Cat No 02CH37283) SECON-02, 2002 Publication	<1%
8	Miveh, Mohammad Reza, Mohd Fadli Rahmat, Ali Asghar Ghadimi, and Mohd Wazir Mustafa. "Power Quality Improvement in Autonomous Microgrids Using Multi-functional Voltage Source Inverters: A Comprehensive Review", Journal of Power Electronics, 2015. Publication	<1%
9	E. Vidyasagar. "Co-Ordination of SVC and on Load Tap Changing Transformer for Reactive Power Control in Power Systems.", International MultiConference of Engineers & Computer Scientists 2008, 20080101 Publication	<1%
10	"New Model of a Converter-Based Generator Using Electrostatic Synchronous Machine Concept", IEEE Transactions on Energy Conversion, 2014. Publication	<1%
11	Yagcitekin, Bunyamin, Mehmet Uzunoglu, Arif Karakas, and Mucahit Vurgun. "Assessment of a car park with electric vehicles", 4th International Conference on Power Engineering	<1%

	Energy and Electrical Drives, 2013. Publication	
12	www.sources4u.com Internet Source	<1%
13	Sao, Charles, and Peter W. Lehn. "Autonomous load sharing between converters and generators in microgrids", 2011 IEEE Power and Energy Society General Meeting, 2011. Publication	<1%
14	www.eco-3.com Internet Source	<1%
15	Kaur, Kuljeet, Amit Dua, Anish Jindal, Neeraj Kumar, Mukesh Singh, and Alexey Vinel. "A Novel Resource Reservation Scheme for Mobile PHEVs in V2G Environment using Game Theoretical Approach", IEEE Transactions on Vehicular Technology, 2015. Publication	<1%
16	bura.brunel.ac.uk Internet Source	<1%
17	ediss.uni-goettingen.de Internet Source	<1%
18	www.bee.qut.edu.au Internet Source	<1%
19	Hui Ren, , Weijun Teng, Chao Jin, and	<1%

Xiaozhou Fan. "Multi-control strategy for the operation of microgrid based on the interior-point method", IET Conference on Renewable Power Generation (RPG 2011), 2011.

Publication

EXCLUDE QUOTES	OFF	EXCLUDE MATCHES	< 7 WORDS
EXCLUDE BIBLIOGRAPHY	OFF		